Modular Radio Frequency Arrays for Microwave Imaging

A Thesis

Presented in Partial Fulfillment of the Requirements for the Degree Master of Science in the Graduate School of The Ohio State University

By

Soumobrata Ghosh, B.Tech

Graduate Program in Department of Electrical and Computer Engineering

The Ohio State University

2023

Master's Examination Committee:

Dr. Steven Bibyk, Advisor

Dr. Emre Ertin

Abstract

Radiofrequency (RF) technology has found numerous medical applications due to its ability to generate heat and create electromagnetic fields. One of the most prominent RF applications in medical industry is detection or monitoring of development of tumor or other diseases in various parts of the human body. However, most of the developed applications are monolithic and not very flexible when it comes to using the same technology for different applications. This thesis presents the design of a scalable board which can be used in creating a modular system that can be used in different applications like detection of lymphedema, pulmonary edema and can also be used to monitor the cardiac muscle activity. We present the basic idea of the board followed by the reason for choosing each component in the board followed by the RF budget calculations and also calculation of several RF parameters like P1dB, IIP3, NF. At the end we present the schematic and layout of the board and also simulation results of the core mixer system at different frequencies.

to Ma and Baba

Acknowledgments

I would like to thank Dr. Emre Ertin who guided me throughout the project. I would like to thank him for giving me the opportunity to be a part of this project. He has been a great motivator and a mentor who has supported me a lot when I have been working as a graduate student in his lab. I feel I have started my journey in being a circuit designer and working in his lab has been the first chapter of this journey. I have learnt a lot of things working with him and working in his lab. I would also like to thank my advisor Dr. Steven Bibyk with whom I took many curses which helped me understand the basics of my field. Working with him has been really crucial in understanding the fundamentals of my field. I would also like to thank my lab mates who are also my friends, Dr. Nithin Sugavanam and Yuyi Chang who helped me throughout this project in many ways. Lastly, I would like to express my gratitude to my parents Debabrata Ghosh and Soumi Ghosh for the way they have supported me and motivated me to pursue this field from my childhood. I am forever indebted to them.

Vita

December 24, 1997 .....Born - Kolkata, India

2020 .....B. Tech Electrical and Electronics Engineering

2022-present .....Graduate Research Associate, The Ohio State University.

Publications

Research Publications

Soumobrata Ghosh, "A robotic system for inspection of railway tracks and like." *Journal of Dairy Science*, 00(2):277–287, Feb. 1900.

Fields of Study

Major Field: Department of Electrical and Computer Engineering

Table of Contents

List of Tables

Table **Page**

List of Figures

Chapter 1: Introduction

Cardiac contractility is the ability of cardiac muscles (myocardium) to contract and generate force during each heartbeat. This contraction of cardiac muscles is essential in circulating blood throughout the body and thus ensuring supply of oxygen and nutrients to all organs and tissues. To have a direct measurement of contractility we need to determine a relation between velocity of myocardial fiber shortening and intra-myocardial tension. [9] . Systolic time intervals (STI) [8] are one of the most successful and simple noninvasive techniques of monitoring cardiac activities. There are three basic STIs namely, pre-ejection period (PEP), the left ventricular ejection time (LVET), and total electromechanical systole (QS). PEP refers to the time interval between the onset of ventricular depolarization and opening of the aortic valve. LVET denotes the time interval between opening and closing of the aortic valve. [10] It is the time during which the left ventricle of heart contracts and ejects blood into the aorta. QS refers to the time interval between the contraction and relaxation of the left ventricle.

This thesis focuses on the development of an array of identical RF blocks which can estimate the velocity of an entire muscular section by collecting and fusing measurements obtained from many locations. Echocardiogram [6] [4] and cardiac magnetic resonance imaging have very similar way of operating [5].

1.1 Background

In this thesis we present the concept idea, design and working of a scalable, modular radiofrequency (RF) block that can act both as a receiver and a transmitter depending on the signal it gets from the control logic. We are using a meander line antenna described in [2] for receiving and transmitting the signal from and to the block, respectively. We would need at least two blocks to collect data for any application. The transmitter block(s) sends electromagnetic waves which hit the target and then gets reflected and gets captured by the receiver block(s) antenna after which we can process the signal to determine the magnitude and phase change of the wave. Depending on the change of magnitude and phase we can comment about different properties of the target. Figure 1.1 shows the block diagram representation of the RF block. A phase locked loop (PLL) is used in the system generate a stepped frequency waveform. In order to have a constant timing across all modules, a clock and synchronization pulse goes through a bus which links all the modules The double pole double throw (DPDT) switch is used so that the same module can act both as a transmitter and receiver. The reference PLL sends the reference signal to the LO port of the mixer. the mixer then down converts the signal to an intermediate frequency (IF) which is then sent through a low pass filter to remove the harmonics and then digitized by the ADC to be processed by the micro-controller. All RF components which include PLLs, mixer, amplifier switch and filters are placed on one board. The digital components which include the micro-controller and ADC are placed on the digital board which is a daughter board to the RF board. The antenna is placed at the bottom of the RF board. Figure 1.2 shows the complete system that monitors the thoracic region, it shows a particular scenario in which the red module is the transmitter, and all other blue modules act as receivers.

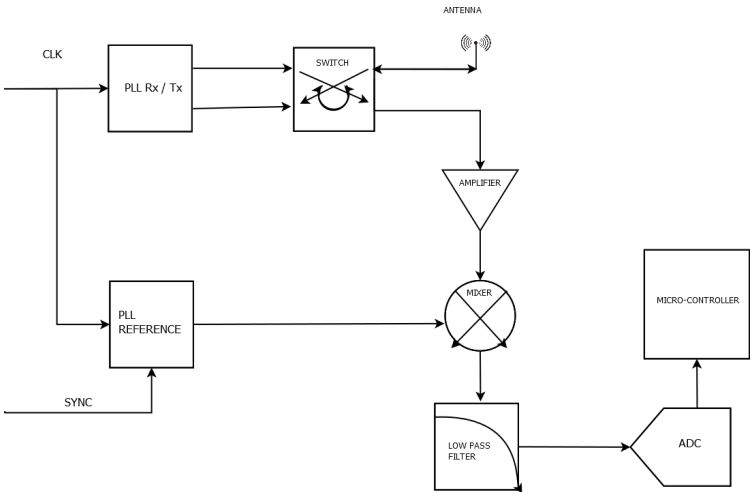

Figure 1.1: Block Diagram Representation of RF board

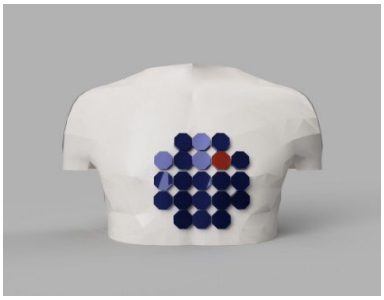

Figure 1.2: Array of identical RF Blocks. This is a scenario where the red module represents the module which acts as a transmitter and all the other blue one's act as a receiver.

Chapter 2: Background

2.1 Radar

A radar, short for Radio Detection and Ranging is a system that uses radio waves to detect, locate, and track objects. A radar transmits electromagnetic waves from a transmitter and then receives the reflected electromagnetic waves from the object being tracked. By analyzing the time, it takes for the waves to travel to the object and back, as well as the frequency shift and phase shift of the waves, the radar system can determine the distance, direction, speed, and even the size and shape of the object. The first detection and ranging by a radar was demonstrated in Britain on June 17, 1935, where the radar was able to detect a flying boat at a range of 27 Kilometers. The present-day sky wave radars have a detection range of 100-3500 Km which says how advanced radars have become nowadays. Nowadays radars are used in aviation, weather forecasting, navigation, defense, and many other applications that require accurate tracking of moving objects.

2.2 Components of a Radar

The main components of a radar are.

1. Receiver
2. Transmitter
3. Antenna
4. Duplexer (switch)

The antenna receives and transmits electromagnetic waves to and from the target depending on whether the radar is acting as a transmitter or a receiver, respectively. The switch output determines whether the radar would be transmitting or receiving signal. The transmitter acts as the signal source when the radar is transmitting, and the receiver processes the data received by the antenna when the radar is receiving the signal. Figure 2.1 shows the block diagram of a simple radar with receiver, transmitter, switch, and antenna. The output from the radar goes to a signal processing unit which determines the distance of the object from the radar.

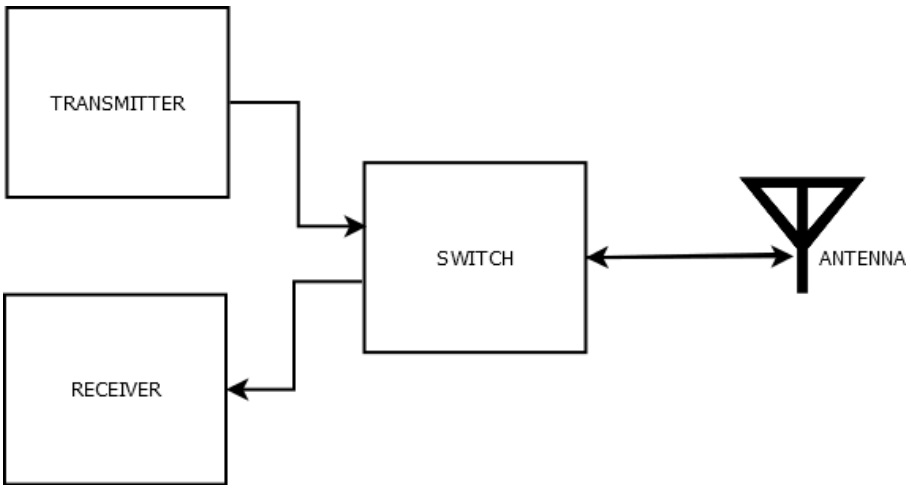

Figure 2.1: A simple RADAR

2.3 Working of a Radar

This section is about the basic working principle of a radar. A device called the magnetron which is inside the radar generates high powered electromagnetic waves which travel in the speed of light. The antenna focuses these waves into a narrow beam. The waves travel in space and hit an object which may be moving or stationary. A part of the energy of the incident waves gets reflected which travels and some of this energy gets captured by the antenna and the data received by the antenna is processed in computers. Based on the strength and the time taken by the waves to travel back the computer can determine the distance between the object and the radar. If there are multiple receivers placed around a particular object, then the signal reflected at different angles by various parts of the object can be used to determine the basic size of the object.

2.4 Determining Position of an Object Using Radar

There are three parameters fundamental for determining the position of an object with a radar.

1. ” The azimuth angle” which is the angle of beam of radar with respect to the perpendicular vector to the ground.
2. ” The elevation angle” which is the angle of beam with respect to the ground.
3. ” Range” which is the straight-line distance between the radar and the object.

When the beam is directed at the object the electromagnetic waves travel a distance of R which is the range before it hits the object. Then the waves are reflected to the radar, and they travel the distance R again until they reach the antenna. So, the waves travel a total distance of 2R. The waves travel at the speed of light. The total time taken by the

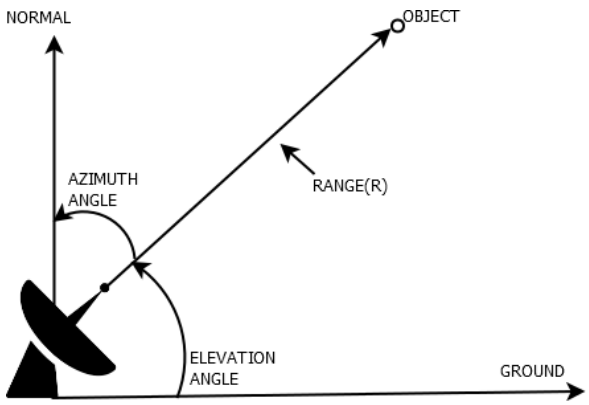

Figure 2.2: 3 parameters for determining position of an object.

radar for determining the position of the object can be represented by T(sec). Figure 2.2 shows the three angles which are the fundamental parameters for determining position of an object using a radar.

$$c = 3 * 10^8 m/s$$

$$2R = c * T \tag{2.1}$$

$$R = c * T/2$$

$$R = 1.5 * 10^8 * T(m)$$

2.5 Determining the Velocity of a Moving Target with Radar

Doppler radars [3] can determine not only the position of an object but also the velocity of an object. Doppler radars transmit pulses of electromagnetic waves which hit the object and then gets reflected to the receiver. By comparing the phase difference of the received

signal with respect to the transmitted signal the velocity and direction of propagation of the object can be determined.

2.5.1 The Doppler Effect

A perfect example of the Doppler effect is the sound of a fire truck heard by a stationary person down the road. The person would observe the sound to become louder and louder as the fire truck approaches and then the loudness decreases as the truck moves away from the person. In addition, the person would also observe the sound to be increasingly high pitched as the truck approaches him and it becomes increasingly low pitched as the truck goes away from him. The sound is the loudest and most high pitched when the truck is closest to the person when the person hears a constant high frequency sound. As the truck goes away from him the observer hears a constant low frequency sound even though the fire truck is producing the same frequency sound all the time. This difference in frequency between the sound transmitted by the truck and the sound heard by the observer is the doppler shift and it depends on the velocity of the truck in this scenario. In figure , the radar transmits electromagnetic waves at the wavelength of l(s) and the object which is moving away from the radar at v m/s speed is receiving the waves at a wavelength of l(o). The electromagnetic waves travel at the speed of light which is represented by c. The frequency of the waves emitted is fs and the frequency of waves received is fo. Time period for source wave is Ts and time period for waves received object is To. Since the object is moving the observed time period.

$$T_o = T_s \pm \Delta t \tag{2.2}$$

The wavelength of the source is given by the distance travelled by the wave in that time plus the distance travelled by the observer which is given by.

$$\lambda_s = \lambda_o \pm \Delta x \tag{2.3}$$

If the object is travelling toward the radar, then the distance travelled by it in that time interval gets added to the observed wavelength and if the object is moving away from the radar, then the distance travelled by the object in that time interval gets subtracted from the observed wavelength.

$$cT_s = cT_o \pm v_o T_o$$

$$cT_s = (c \pm v_o)\ To$$

$$\frac{c}{f_s} = c \pm v\frac{1}{f_o}$$

$$f_o = f_s\ \frac{c \pm vo}{c})$$

$$(\quad f_o = f_s (1 \pm \frac{v_o)}{c} \tag{2.4}$$

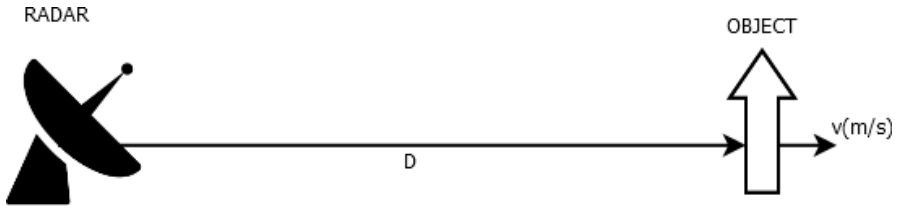

Figure 2.3: The Doppler Effect

In equation 2.5 the fo is the frequency received by the object. After the object gets hit by the electromagnetic waves it reflects the waves and the waves travel the same distance again until it gets received by the radar. The frequency that the radar will receive now is.

given by

$$f_r = f_s(1 \pm \frac{v_o}{c})^2 \tag{2.5}$$

$$f_r = f_s(1 \pm 2\frac{v_o}{c} + \frac{v_o^2}{c})$$

Now since vo is much less than c, so we can ignore the last term to rewrite the equation.

$$f_r \approx f_s(1 \pm 2\frac{v_o}{c}) \tag{2.6}$$

Thus, the frequency of the echo signal received by the radar and the signal transmitted can be linked by the following equation.

$$f_r = f_s(1 \pm 2\frac{v_o}{c})$$

$$f_r = f_s \pm 2\frac{f_s v_o}{c} \tag{2.7}$$

The last term in equation 2.8 is what is known as the doppler frequency (fd).

$$f_d = 2\frac{f_s v_o}{c} \tag{2.8}$$

The radial velocity of the object can be calculated from equation 2.9 which is given by the following equation,

$$v_o = \frac{f_d c}{2 f_s} \tag{2.9}$$

2.6 VNA Functionality of the Scalable RF Board

In this section we are going to explain about the working principle of a VNA and how it gives a higher resolution of the data provided by the scalable RF board. A VNA (Vector Network Analyzer) is an instrument used to measure the electrical characteristics of radio frequency (RF) networks. It generates a radio frequency signal and then measures the amplitude and phase of the signals that are transmitted and received by the device under test. The impact factor for a VNA is that it can measure both magnitude and phase. If someone needs to measure just the magnitude, he or she can do that with much simpler, less complicated, and less expensive equipment like the scalar network analyzer. The VNA typically consists of a signal generator that generates a swept or stepped frequency signal, which is sent through a directional coupler or other device to the device under test. The reflected signal from the network is then measured by the VNA using a detector or other sensing mechanism. The VNA then uses this information to calculate the magnitude and phase of the reflection coefficient, which describes how much of the signal is reflected from the device under test, which tells us about the dielectric properties of the material. The VNA can also measure the transmission coefficient, which describes how much of the signal is transmitted through the device, as well as the phase shift and other properties of the device. This information can be used to characterize the performance of the network, diagnose problems, and optimize the design of the network for specific applications. So, a VNA works by generating a radio frequency signal and measuring the signals that are transmitted and reflected by the device under test, and then using this information to calculate various electrical characteristics of the device. Now we will discuss the reflection and transmission parameters measure by the VNA.

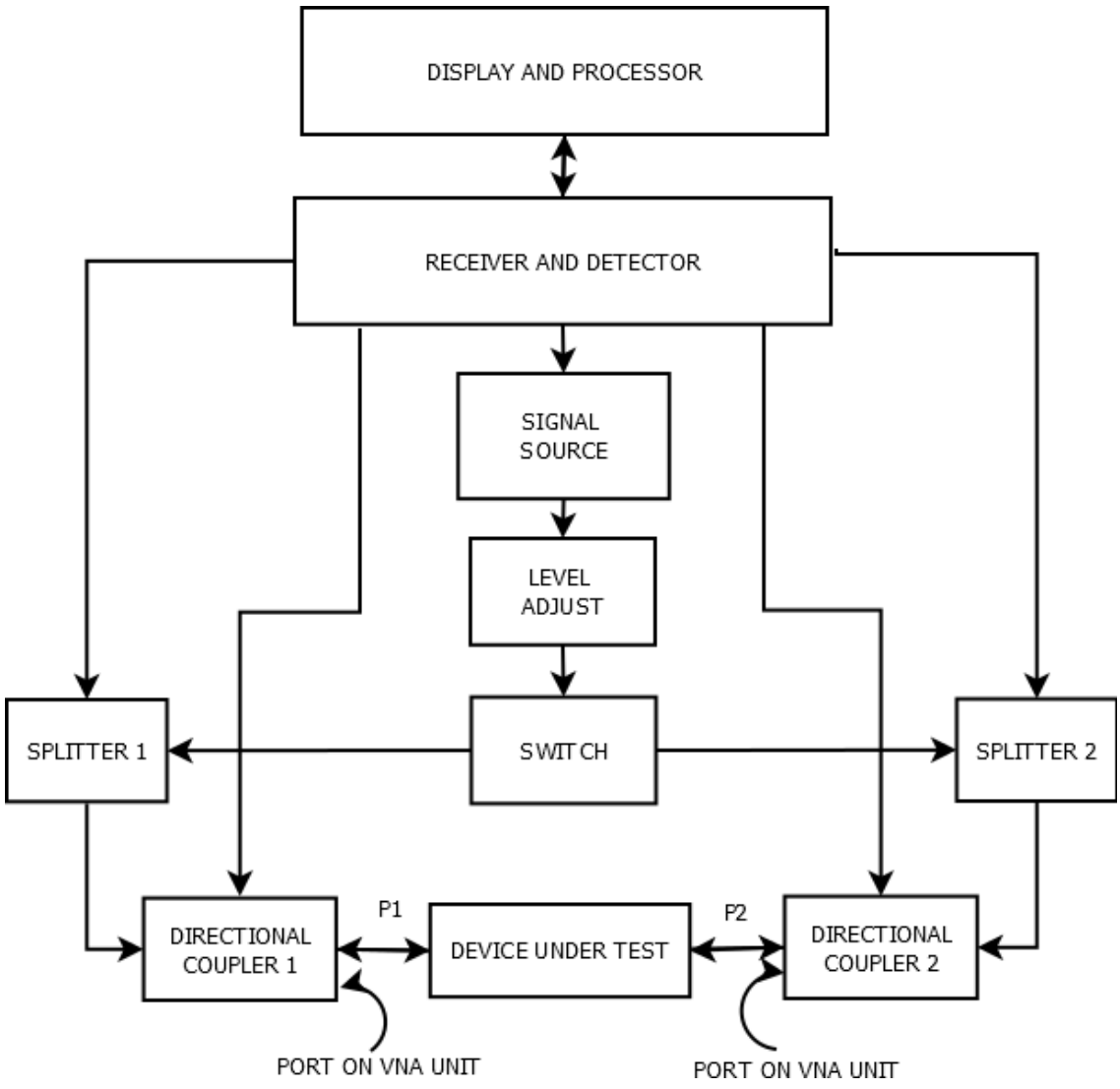

Figure 2.4: Block Diagram Representation of A VNA

Transmission and Reflection Parameters:

$$\tau = V_{reflected} / V_{incident} \tag{2.10}$$

$$= (Z_L - Z_0) / (Z_L + Z_0), \tag{2.11}$$

$$Returnloss(R) = -20log(\rho) \tag{2.12}$$

$$TransmissionCoefficient\,(T) = V_{transmitted} / V_{incident} \tag{2.13}$$

$$InsertionLoss = 20log\,(T) \tag{2.14}$$

$$V_{reflected} = voltageofthereflectedwave$$

$$V_{incident} = voltageoftheforwardorincidentwave$$

$$Z_L = loadimpedance$$

$$Z_0 = matchingimpedance$$

(2.15)

Figure 2.4 shows the block diagram of a network analyzer. Now we will discuss the working of the scalable RF board. The board can act both as a receiver and a transmitter.

To collect the data, we need at least two boards one acting as a transmitter, the other acting as a receiver. The transmitter sends electromagnetic waves to the tissue. The electromagnetic waves get reflected from the tissues and the receiver receives these waves. Comparing the magnitude and phase of this reflected waves with that of the incident waves sent from the transmitter we can comment on the dielectric properties of the tissue. The scalable RF board thus has the same working principle as that of a VNA. The difference is the calibration flexibility that one can get while using a VNA.

2.7 Proposed Modular Architecture

The final system as said in the introduction will have an array of modules, where each module is the RF board. All these modules will have three common signals which are the ground, reference, and the synchronization signals. The ground is for reference. The reference signal is a digital clock for the PLLs. The synchronization signal is for synchronizing the reference PLL in each module. Figure 2.5 shows 9 modules in the system. The RF board block diagram shown in introduction is also there in each module in figure below. The three common signals, ground, reference, and synchronization signals go through all the modules. This is how the modularity of the board can be demonstrated.

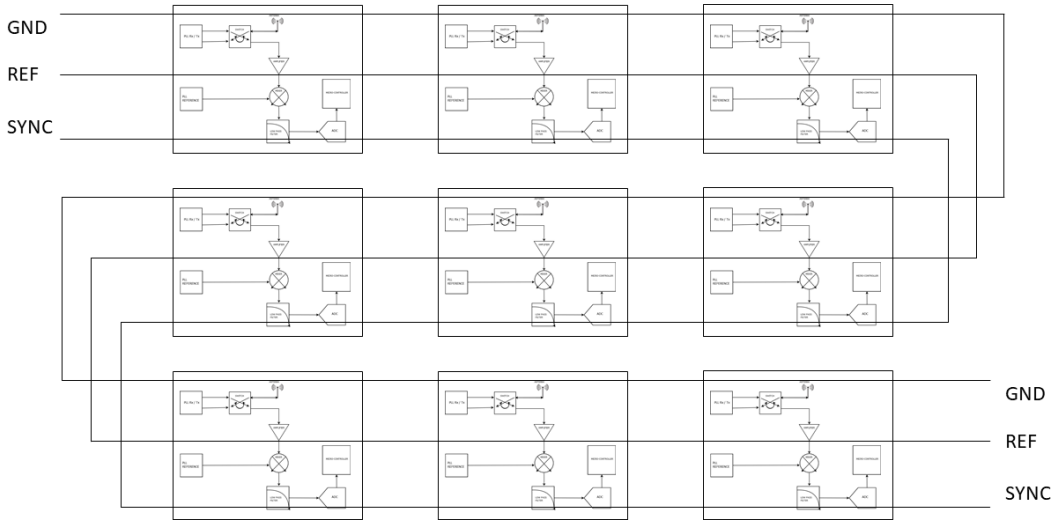

Figure 2.5: Diagram Representation of the modular system

2.8 Scalability of the Proposed Design

One of the key features of the RF board as the name suggests is the scalability. Depending on the application the system can be made bigger or smaller by having more or less modules whichever the application demands. For monitoring the cardiac activity as shown in figure 1.2 we can see a huge array of modules wrapping the thoracic cavity. For detection of lymphedema on the other hand there is a much smaller array of only two modules per row forming a band to cover the entire arm as seen in figure 2.6. For brain tumor detection there is again a different arrangement of modules as can be seen in figure 2.7 . There are several strands covering the brain with each strand having three modules. Thus, we can have different arrangement of modules according to our need or according to whatever the application demands.

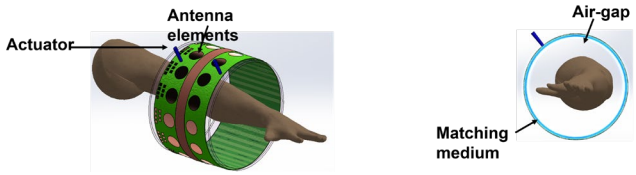

Figure 2.6: The sensor system comprising of RF scanning system to compute tissue composition and Limb-volume for detection of lymphedema.

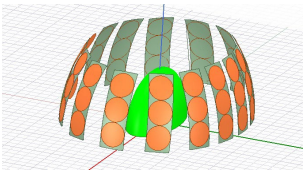

Figure 2.7: Sensor system for Brain Tumor Detect

Chapter 3: Design Specifications for the RF Board

In this section we would first discuss the basis of selecting all the circuit elements we have in the RF board. We would go through all the specifications of all the components one by one. After that we would go through different calculations like RF budget analysis for when the system acts as a transmitter as well as a receiver, noise figure of the system, 1db compression point of the system and third order input and output intercept point.

3.1 Phase Locked Loops (PLLs)

The primary building block of the RF board are the two-phase locked loops (PLLs) which are used to generate signals of required frequencies. In our application we are operating in the frequency range of 500MHz to 4GHz. MAX2871 is capable of generating frequencies between the ranges of 23.5MHz to 6000 MHz We are mixing the signals from the main PLL and the reference PLL to get an intermediate frequency (IF) signal which is further digitized and processed by the micro-controller. The PLLs however have harmonics which gets mixed to each other causing distortion. To filter the harmonics, the IF signal is passed through filter to attenuate the harmonics to an extent where they have very low power. To know how much attenuation needs to be given to the harmonics by the filter we need to know the actual power levels of the harmonics produced by the PLLs. According to the data sheet the fundamental VCO output should have the second and third harmonic values.

as -40 dBc and -34 dBc, respectively. Also, if the VCO output is divided by two the second and third harmonics should be -25 dBc and -20 dBc, respectively. We connected the MAX2871 evaluation kit to Agilent Technologies N9030A PXA Signal analyzer. We observed the power levels of the harmonics in the RF power spectrum for the frequencies of 0.6GHz, 1GHz.

, 2GHZ, 3GHz and 4 GHz. The power levels of the harmonics that we observed are given in the table 3.1 . In the results section the simulation results that we show are considering these observed power values of second and third harmonics given in table 3.1. Figure 3.1 shows the output power spectrum of the PLL, MAX2871 at different frequencies.

Frequency (In GHz)	Second Harmonic (In dBc)	Third Harmonic (In dBc)
0.6	31.11	9.2
1	23.09	8.42
2	24.7	13.7
3	27.35	25.65
4	33.6	30.8

Table 3.1: PLL Harmonics

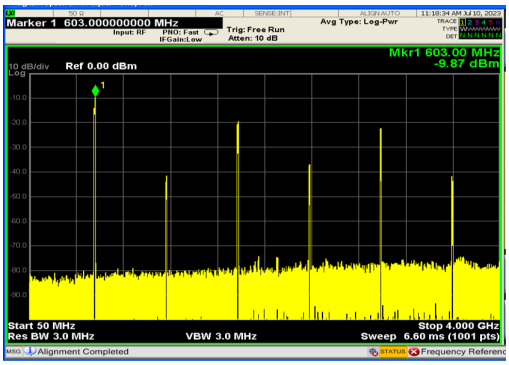

(a) PLL output at 0.6 GHz

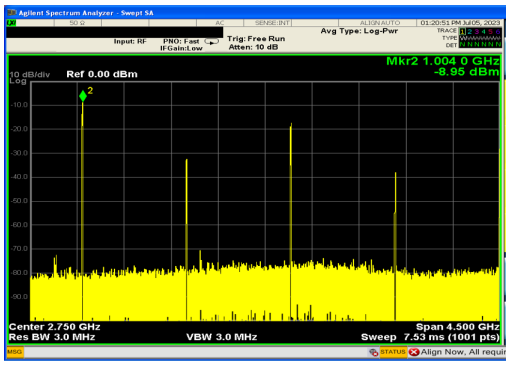

(b) PLL output at 1 GHz

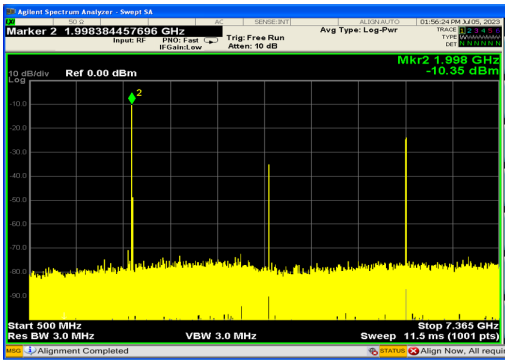

(c) PLL output at 2 GHz

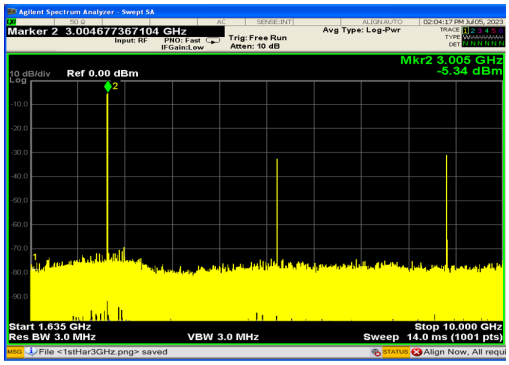

(d) PLL output at 3 GHz

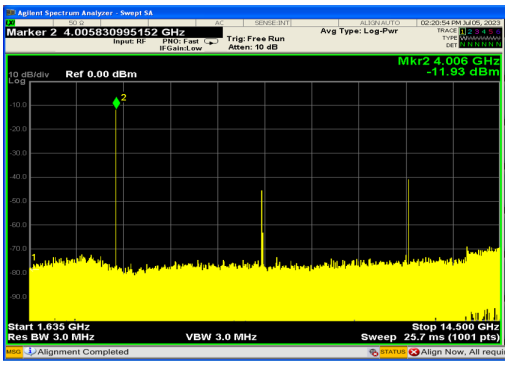

(e) PLL output at 4 GHz

Figure 3.1: PLL Harmonics at Different Frequencies

3.2 Double Pole Double Throw (DPDT) Switch

For the module to work both as a receiver and a transmitter depending on the control signal output, we need to have a double pole double throw switch which has two RF input ports (Rx and Tx), two RF output ports (A1 and A2), two control voltages (V1 and V2). The two RF ports are connected to two separate circuits one for the receiver and one for the transmitter. Depending on the input received by the control voltage terminals it will complete the receiver or the transmitter circuit. The V1 and V2 lines are connected to the micro-controller for control input, they are however not shown in figure. The PLL has two outputs which deliver the same signal. The two outputs of the PLL are connected to the Tx and A2 ports. The A1 port is connected to the antenna. The Rx port is connected to the amplifier. When the module acts a transmitter, Tx gets connected to A1 which sends the PLL signal through the antenna. A2 gets connected to Rx which delivers the PLL output to the mixer RF port after which it gets digitized and then sent to the micro-controller. When the module acts as a receiver, A1 gets connected to Rx which allows the antenna to send the received signal to the RF port of the mixer after which it is again digitized and sent to the micro-controller. The Tx port is connected to A2. The RF enable line coming from the micro-controller is disabled in this scenario which disables the RF output coming from the two PLL ports. Table 3.2 demonstrates the working of the DPDT switch in detail.

V1	V2	A1-Tx	A1-Rx	A2-Tx	A2-Rx	RF Enable
0	1	connected	isolated	isolated	connected	1
1	0	isolated	connected	connected	isolated	0

Table 3.2: DPDT switch working demonstration.

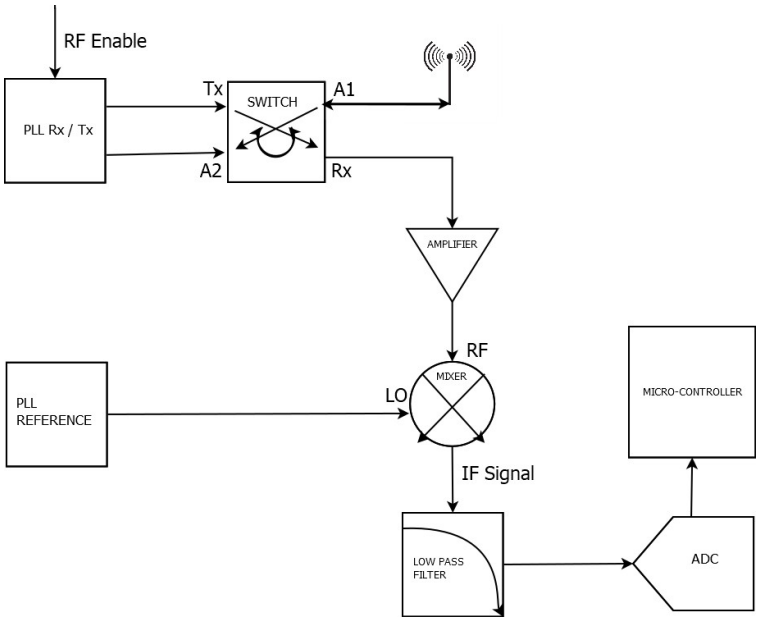

Figure 3.2: Working of DPDT switch.

3.3 Mixer

We would be using ADE-30W+ mixer in our application. The mixer is operational in our application range of 0.5 GHz to 4 Ghz. The MAX2871 PLL which we are using can deliver programmable output differential power from -1dBm to 8dBm across its two output ports, which means each output can be programmed to deliver output between 0dBm to 5dBm. The mixer LO port is connected to the reference PLL. The reference PLL will be programmed to deliver 4dBm of power which sets the LO power to 4dBm for the mixer. The performance data given in the manufacturer's website show the 1dB compression point and the conversion loss of the mixer with 4 dBm input power for different frequencies. In the simulation results shown in the results section we configured the mixer according to the data provided in the performance data given by the manufacturer. For the RF budget calculations, we would be assuming the worst-case situations of the mixer to

demonstrate our calculations. We would assume the mixer to have a gain conversion of 8.66 dB and a 1 dB compression point of 0.36 dB which are the worst-case scenario values. For the AWR simulations in the results section we would be configuring the mixer for each frequency to update the gain compression and 1dB compression point values.

3.4 Low Pass Filter

The IF signal output from the mixer needs to be passed through a low pass filter to attenuate the harmonics at higher frequencies. Since we have an offset of 25KHz from the Rx/Tx PLL, the signals at frequencies higher than 25KHz needs to be attenuated and for that we would need a 25 KHz low pass filter. Initially we chose LTC1563-2 which is an active fourth order RC Filter. The macromodel of LTC1563-2 was available in LT spice. We did an ac simulation of the reference circuit provided in the datasheet to get the magnitude and phase response of the filter. The application circuit is shown in figure. The ac simulation response results are shown in figure. The cut-off frequency of the filter is given by 3.1

$$f_c = 256(10k/R)\ kHz \tag{3.1}$$

Since we need to set the cut off frequency to 25 kHz, we chose the value of R to be 100k. So, the cut off frequency is set to 25.6 kHz. The ac response at 50kHz and 75kHz are -22dB and-36 dB respectively, which means the second and third harmonics are attenuated by that value. But we need at least 40dB of attenuation for the second harmonic. So, we needed to have a filter of higher order and more stages. We used analog electronics filter wizard to see how many stages we need for having the required attenuation at 50kHz. We needed to have as a smaller number of stages as possible as more stages would mean a greater number of amplifiers as buffers which would make laying out the components.

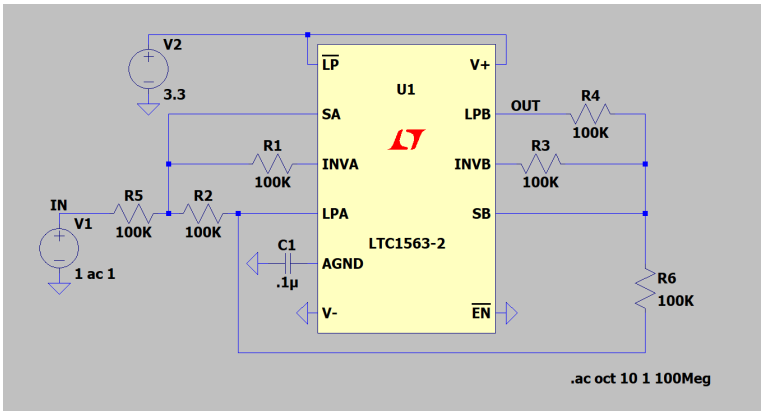

Figure 3.3: LTC1563-2 Simulation Setup from Macromodel in LT SPICE

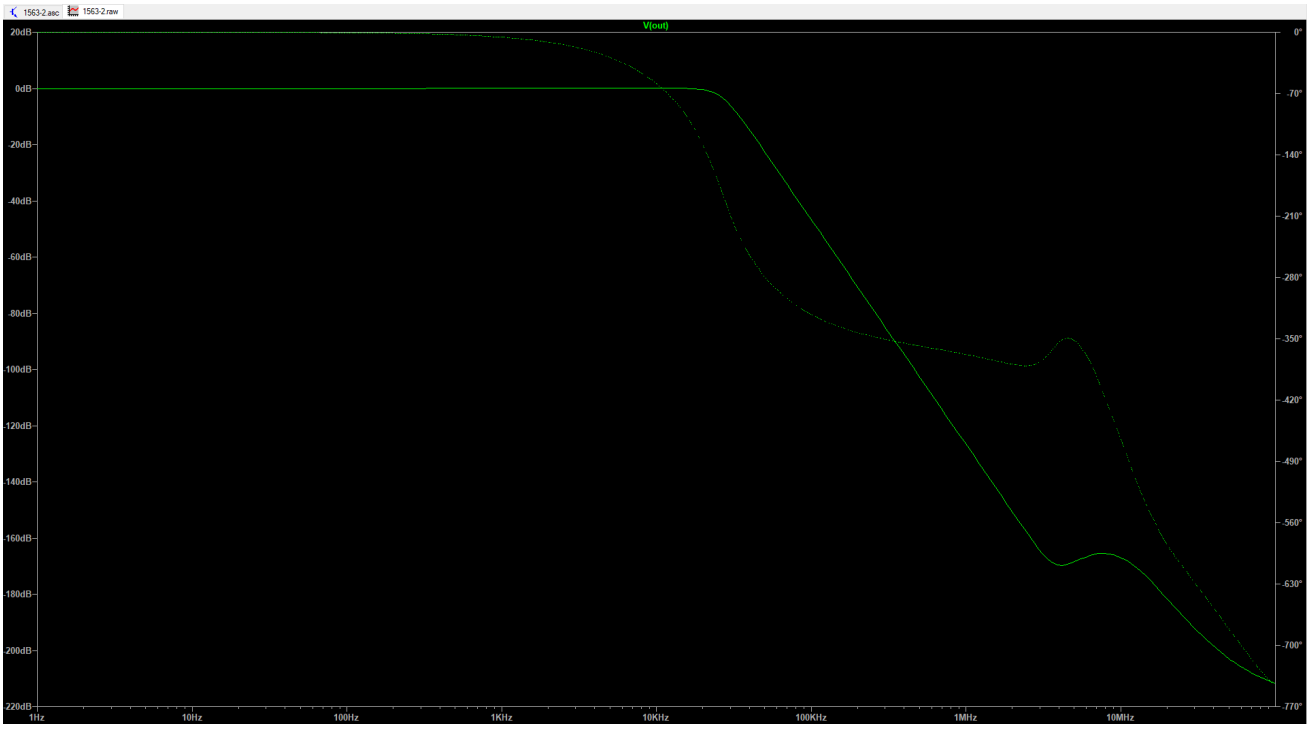

Figure 3.4: AC Simulation Response for LTC-1563-2. Solid line represents magnitude response. Dotted line represents phase response.

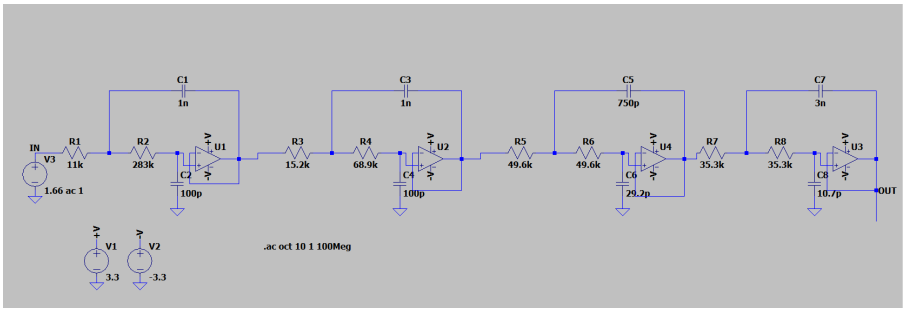

Figure 3.5: OP484 Simulation Setup from Macromodel in LT SPICE

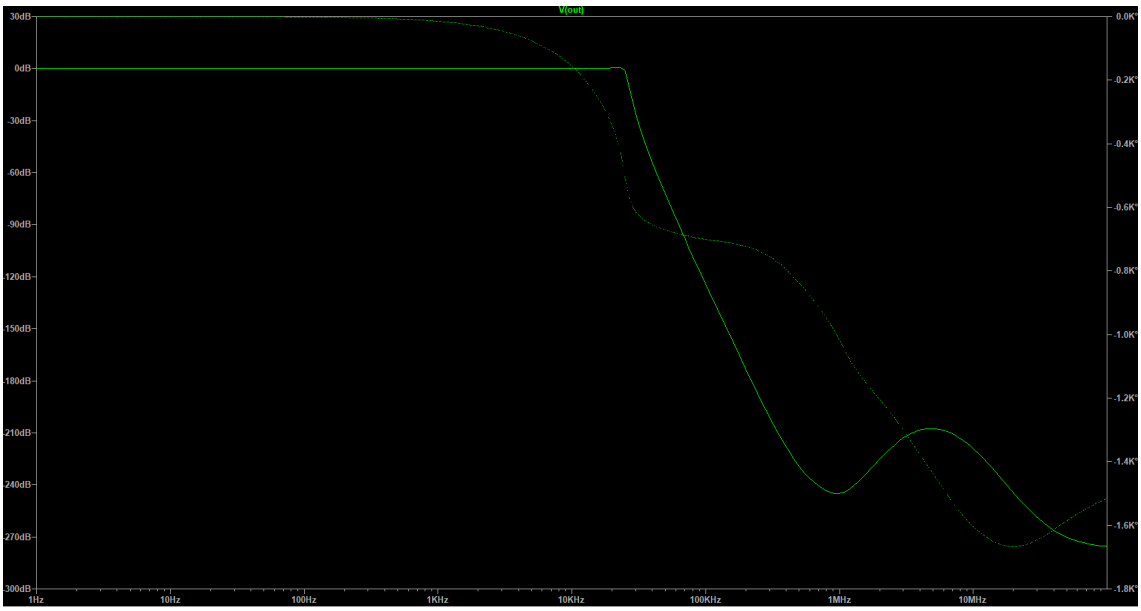

Figure 3.6: AC Simulation Response for OP484. Solid line represents magnitude response. Dotted line represents phase response.

even more challenging as there is a constraint of space. We chose an eighth order Chebyshev filter with three stages. The simulation setup and ac response for this filter is shown in figure 3.6. The eighth order Chebyshev filter uses sallen-key topology and the amplifiers used for buffer is OP484. The ac response showed a magnitude response of -70.2dB at 50KHz and -103 dB at 75 kHz which is sufficient attenuation for the second and third harmonics.

3.5 Amplifier

We would be using SKYA21051 Low Noise Amplifier (LNA) in our module. The LNA has a bandwidth from 200 MHz to 6000 MHz which falls in our application frequency bandwidth. The amplifier also has a flexible bias voltage from 3V to 5 V. We would be biasing it to 3.3 V in our design. The bias voltage will be supplied by an LDO which will be discussed in later sections. The amplifier has a maximum gain of 17.8 dB at 700 MHz and lowest gain of 14.5 dB at 4000 Mhz. The LNA has low noise figure of 1 dB. However, the NF values changes with frequency, and it increases to a maximum of 1.3 dB at 3800 MHz as shown in the application circuit in the data sheet we would be placing a dc blocking capacitor both at the RF input and output ports to block the dc harmonics.

3.6 Power Management

In this section we are going to discuss the basis of choosing the power management components for the board.

3.6.1 Low Drop Out Regulator (LDO)

The filter and the amplifier that we are using both require a constant voltage supply of 3.3 V. So, we need to use a LDO in the board which is going to give the constant supply voltage of 3.3 V to both the components. Also, this LDO should supply the minimum current requirements of both the devices. The filter (LTC-1563-2) typically needs 8 mA of supply current. The amplifier (SKYA21051) needs 100 mA of supply current which is adjustable. So, we would need at least 108 mA of supply current from the LDO. We chose TPS7B81 which can supply 150 mA of current and can also supply 3.3 V. It also has ultra-low I_q. The dropout voltage is 180mV.

3.6.2 Connector

The LDO needs a power supply externally and the RF switch used also needs two digital voltage V1 and V2 which is used to control the switch. The LDO input voltage and the dc voltages needed by the switch will be supplied externally through a male connector (5031590501) which is placed on the board. It has five pins. We would be using just three for supplying power to the board.

3.7 Analog to Digital Convertor (ADC)

The IF signal coming out of the mixer is 25 kHz. So, to sample that signal we would need an ADC with sampling rate of at least 50 kHz. We chose AD7980 which is a 16-bit ADC with a sampling rate of 1 MSPS which is 1 Mega sample per second. However, we would be operating it at a sampling rate 187kHz which is above the Nyquist rate. It has an SNR of 91.5 dB. Equation (3.2) shows the effective number of bits (ENOB) of the ADC.

$$ENOB = \frac{SNR\,(dB) - 1.76}{6.02} = 14.9 \tag{3.2}$$

Thus, the effective number of bits of the ADC is 14.9 bits.

3.8 Antenna

In our RF module we would be using a flexible meander line antenna array shown in [1]. The antenna is operational in our application frequency band from 0.5GHz to 4Ghz. At first there is a matching layer of thickness 3.25mm which in our application is the Roger 3006 dielectric material with a dielectric constant of 6.15. After that there is the copper radiating element which acts as the transmission line. There is a dual section of meander line in this antenna. The reason for having a dual section is to have bigger bandwidth. After that there is 10mm silicon layer and then there is the ground plane. Below the ground plane there is a SMA connector which is connected to the RF board which delivers the power to the antenna when the module is acting as a transmitter, and it delivers the power received by the antenna to the module when the module acts as a receiver. We have two vias, one connecting the transmission line to the module via the SMA connector for power supply or delivering and the other via connects the other end of the transmission line to the ground plane. The SMA connector is made of brass with a Teflon insulator going through it. In the HFSS simulations we have placed two antennas one acting as transmitter and one acting as receiver. The two antennas are placed at a distance of 15mm. The two antennas are on top of different layers we have placed for emulating the human skin. The dielectric constant of all these layers is set to be frequency dependent. At first there is the dry skin layer of 1mm thickness, followed by the fat layer of 20mm thickness, which is followed by the muscle layer of 10 mm thickness. After that there is the bone layer of 5mm thickness followed by the lung in deflated stage of 30mm thickness. Figure 3.7 shows the HFSS setup for running antenna simulations.

We ran a frequency sweep of 501 points from 100 MHz to 5Ghz to get the s11 and s12 responses of the antenna. Figure 3.9 shows the s11 and s12 responses for the antenna. The

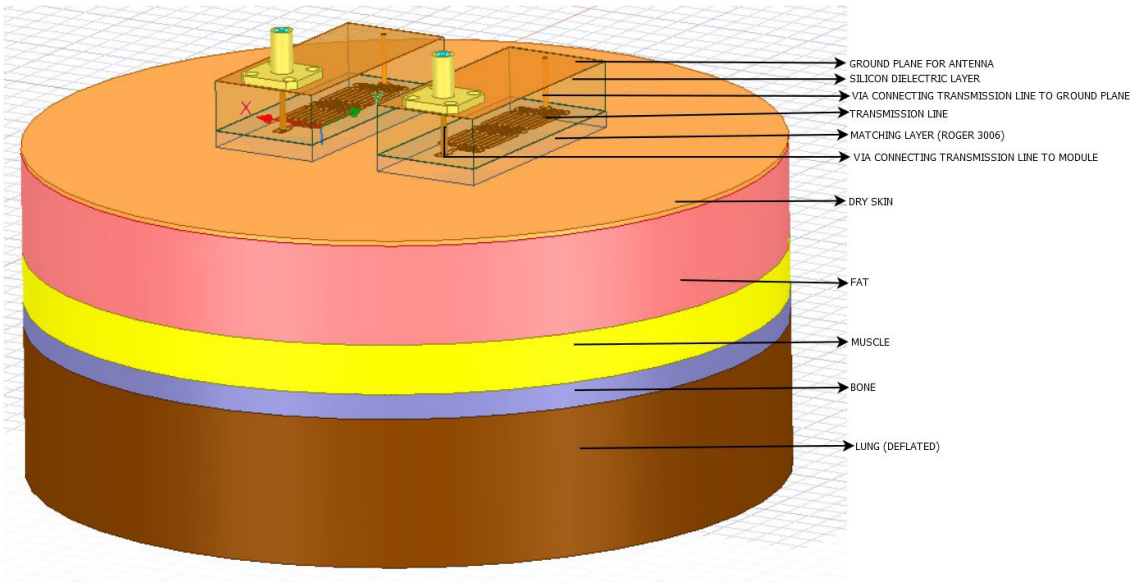

Figure 3.7: HFSS Setup for Antenna

s11 seems to have an average value of -10dB. the s12 seems to have an average value of -30dB. Since we would be sending 5dBm of power from the transmitter module PLL, that means the antenna at the receiver module would get -25dBm of power. These values are used in the RF budget analysis section to determine the power we would be sending to the system.

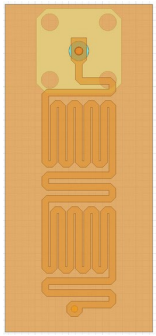

Figure 3.8: Meander Line antenna

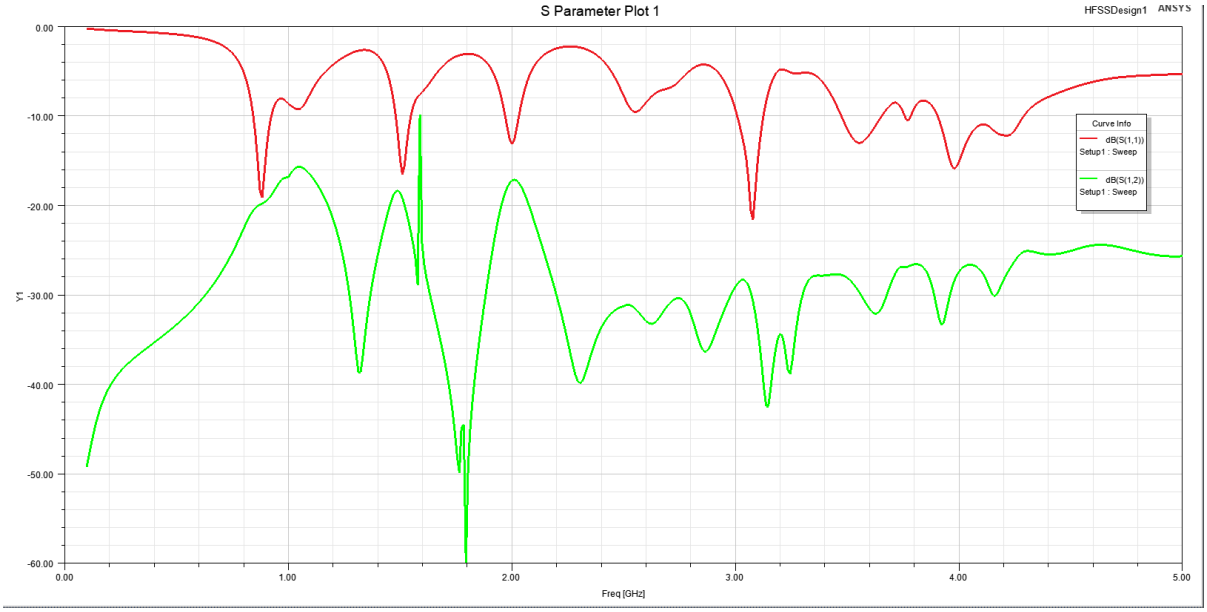

Figure 3.9: HFSS Simulation Results for Antenna

3.9 Micro-strip Calculations

When routing the conductor on the first layer of the board to connect different components, the width of the conductor needs to be such so that the conductor is matched to 50 ohms to avoid any mismatch loss. Figure 3.10 shows the conductor on top, then the dielectric layer in blue followed by the second conductor layer in the board which acts as RF ground for this board. The conductor thickness (t) is 1.2 mils. The dielectric layer thickness.

(h) is 8 mils and the relative permittivity of the dielectric layer is 3.55. Using (3.3) the conductor width is 13.2984 mils or 0.3378 mm.

w = *conductorwidth*

h = *dielectricheight*

t = *conductorheight*

$$w = \frac{7.48h}{e^{\frac{\sqrt{\varepsilon_r + 1.41}}{87}}} - 1.25t \tag{3.3}$$

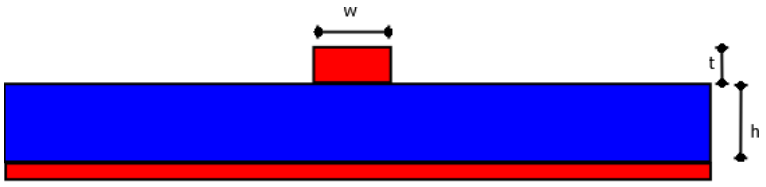

Figure 3.10: Microstrip

Chapter 4: Analysis of the Design

In this chapter we would be demonstrating RF budget analysis for the module for both the cases of when it acts as a transmitter and when it acts as a receiver. For amplifier gain we would be considering the maximum gain of 17.8 dB. For mixer p1dB and gain compression we would be considering the values of 0.36dB and 8.66dB respectively which are the worst-case scenario values. We would also calculate the cascaded gain, IIP3, P1dB, NF of the system.

4.1 When Module acts as a Receiver

In this section we will demonstrate the RF budget analysis of the module when it acts as a receiver. When the RF module acts as a receiver the two PLL outputs connected to the switch ports Tx and A2 gets connected. The PLL is however disabled by the RF Enable line. The reference PLL connected to the LO port of the mixer is delivering a power of 4dBm to the LO. The antenna signal goes through the switch to the amplifier. The A1 and Rx terminals of the switch get shorted. From the observed s12 values of the antenna in HFSS simulations we can say the antenna has an average s12 of -30dB. When the module acts as transmitter, we are sending 5dBm of power from the antenna, which means the receiver antenna will be getting -25dBm of power. The -25dBm received signal from the antenna then goes through a 0.6dB switch loss to have -25.6 dBm input power to the

amplifier. The highest gain the amplifier has is 17.8 dB. The mixer has a 1 dB compression point of 0.34 dBm for 4 dBm LO power in worst case. So, The amplifier output signal cannot be more than 0.34 dB. If the amplifier gain is 17.8 dB, then the mixer input would be -7.8 dBm which would not saturate the mixer. The mixer has a worst-case gain conversion of 8.66 dB which means the power entering the RF port will be reduced by 8.66 dB when it leaves the IF port. Thus, the mixer output power will be -16.46 dBm which corresponds to 92mV peak to peak. Figure 4.1shows the budget analysis for the module acting as a receiver.

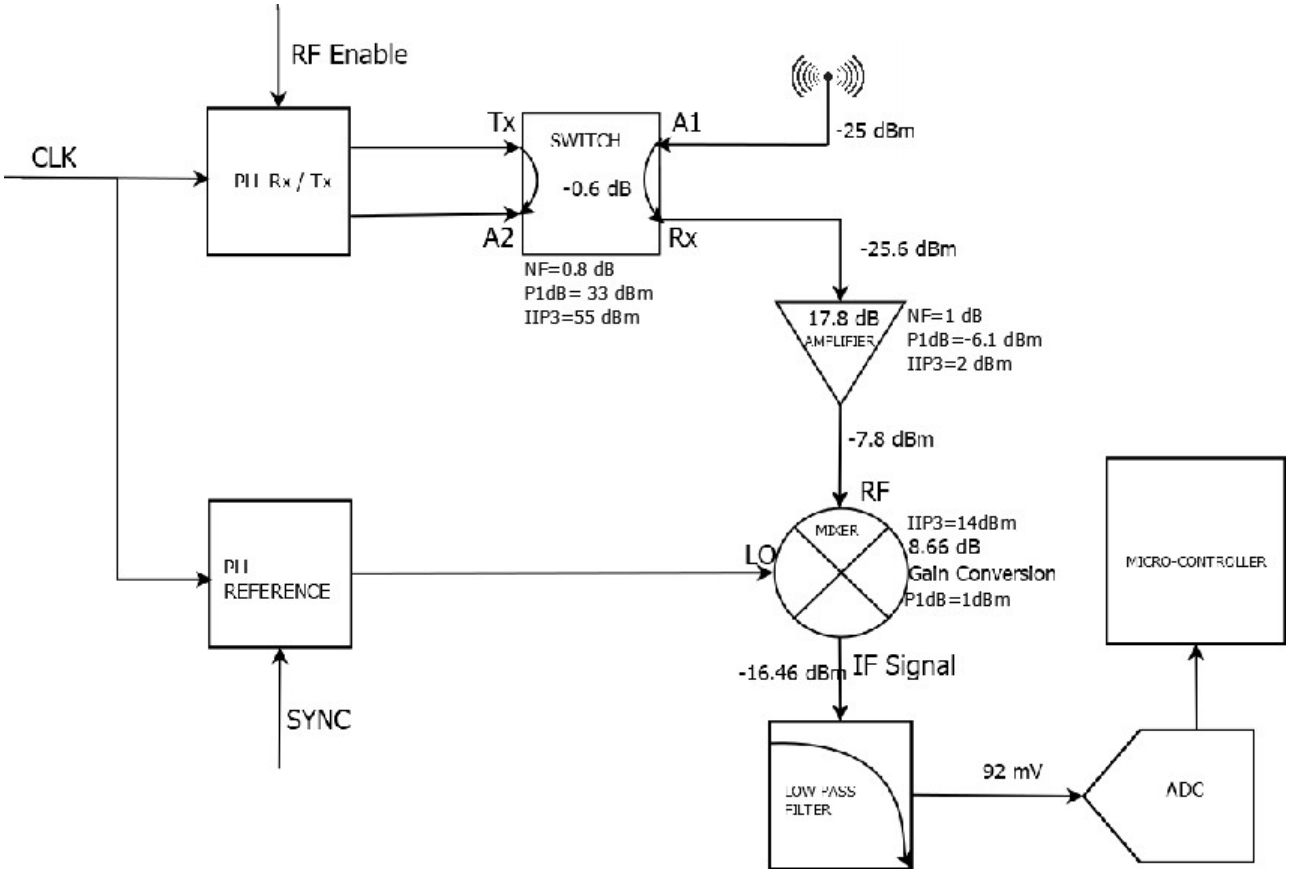

Figure 4.1: RF Budget Calculations for when module acts as a receiver.

4.2 When Module acts as a Transmitter

In this section we will demonstrate the RF budget analysis of the module when it acts as a transmitter. In the DPDT witch Tx is connected to A1 and A2 is connected to Rx. The RF enable line enables the PLL when the module is acting as a transmitter. One output of the PLL which is connected to the Tx port of the switch, is connected to the antenna through the switch. That PLL output is programmed to have an output of 5dBm. After having a switch insertion loss of 0.6 dB, 4.4 dBm of power is being transmitted through the signal. The other output of the PLL is however connected to the amplifier through the switch. The PLL can be programmed to deliver a minimum power of -4 dBm through this output. If this

-4dBm signal goes through the switch it would be a -4.6 dBm input signal for the amplifier. Since the amplifier has 17.8 dB gain, it would be 13.2 dBm input signal to the mixer which would saturate the mixer as the mixer has 1 dB compression point of 0.34 dB. To solve this problem, we would be placing an attenuator right after the output of the PLL which is connected to the amplifier. If we place a 14 dB attenuator between that output of the PLL and the switch that would make the amplifier input signal -18.6dBm. Passing through the 17.8 dB gain amplifier it would be -0.8 dBm input signal to the mixer. The mixer has a gain conversion of 8.66 dB. Thus, the mixer output would now be -9.46dBm. Figure 4.2 shows the budget analysis for module acting as a transmitter.

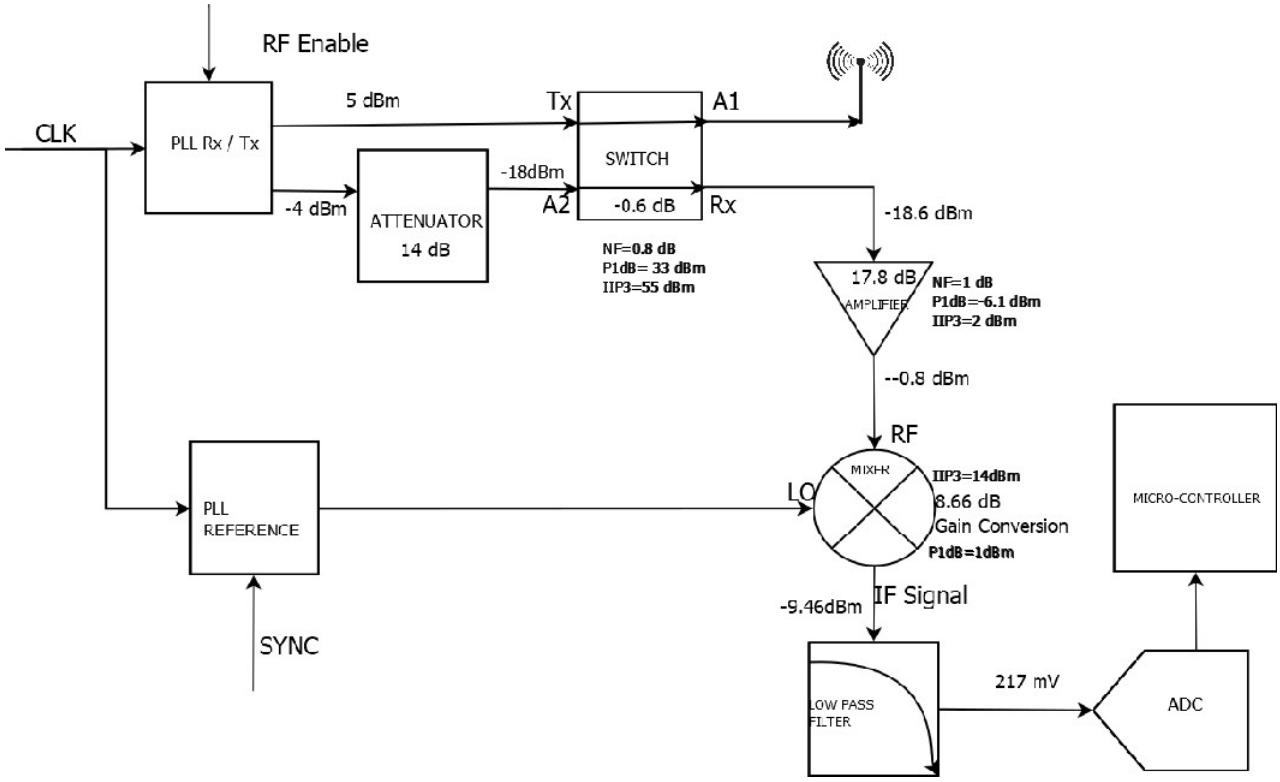

Figure 4.2: RF Budget Calculations for when module acts as a transmitter.

4.3 SIMULINK Simulation Results for RF Budget Analysis

The RF chain shown in section 4.4 was imported in SIMULATION to run a simulation to verify the mixer output power in both cases. Components shown in blue represent the RF components, switch, amplifier and mixer. The first element named RF element is a generic RF block we used to emulate the switch. The second block is the amplifier. The third block , demodulator is the mixer which is operating in down-conversion mode. Figure 4.3 shows the receiver scenario in which -25 dBm of input power was given to the system. The output of the system is -16.55 dBm which is same as what we found in our calculations. Figure 4.4

shows the transmitter scenario in which -18 dBm of input power is given to get -9.88 dBm of power which is same as what we calculated in the previous section.

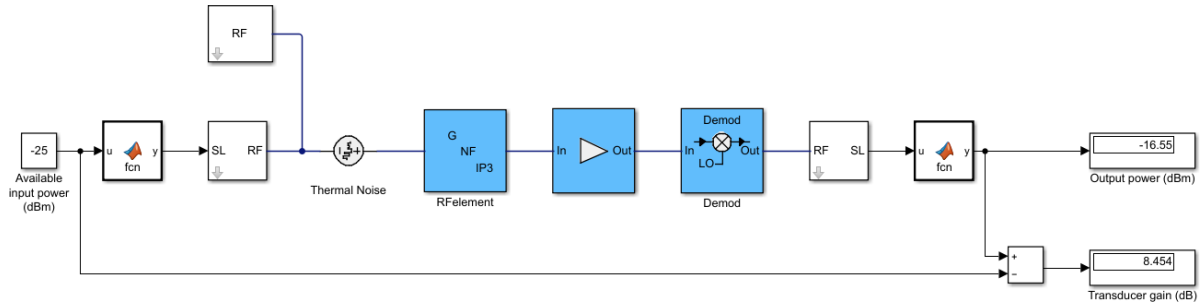

Figure 4.3: Receiver Simulation Results

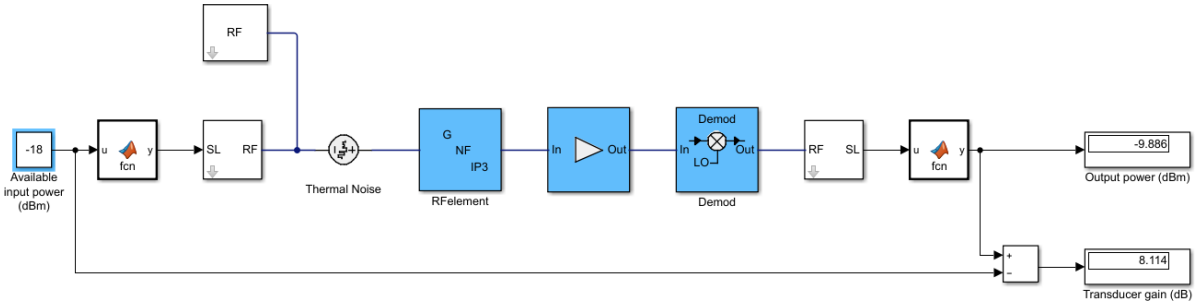

Figure 4.4: Transmitter Simulation Results

4.4 Cascaded Gain, NF, IIP3 and P1dB

In this section we would be finding the cascaded gain, NF, IIP3 and P1dB values of the RF chain shown in figure 4.5 consisting of switch, amplifier and mixer. The specifications given in table 4.1 will be used to find the cascaded values. The specifications are taken from the datasheet of the respective components considering worse case scenarios. The mixer noise figure is same as the gain conversion of the mixer. The noise figure of the switch is same as the insertion loss. The cascaded P1dB, NF, gain, IIP3, OIP3 equations given below establish a relationship between the characteristics of each individual components and the cascaded characteristics of the system. However, all the values in dB or dBm was converted to linear values before putting them in the equations below.

Component	Gain (In dB)	NF (In dB)	IIP3(In dBm)	P1dB (In dBm)	OIP3(In dBm)
Switch	-0.6	0.8	55	33	54.4
Amplifier	17.8	1	2	-6.1	17
Mixer	-8.66	8.66	14	1	5.34

Table 4.1: Component Specifications

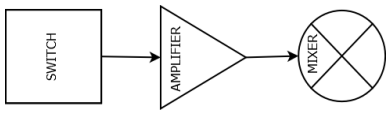

Figure 4.5: RF Chain

4.4.1 Gain

The cascaded gain of the system can be found simply by adding the gain of all the components in the system. The cascaded gain G can be given by the equation 4.2

$$G_{cascaded} = G_{switch} + G_{amplifier} + G_{mixer} \tag{4.1}$$
$$= -0.6dB + 17.8dB - 8.66dB$$
$$= 8.54dB$$

So, the cascaded gain of the system is 8.54 dB.

4.4.2 1dB Compression Point (P1dB)

P1dB or the 1dB compression point of a device is the input power at which the device starts to act nonlinearly. However, the cascaded p1dB gives us an idea about the saturation input power of the system. The cascaded p1dB equation is given by equation 4.3. Noise figure of mixer is considered to be equal to its conversion loss. Noise figure of switch is. considered to be equal to its insertion loss.

$$P1db = 10log_{10}\left[\frac{1}{\frac{P1dB_{switch}}{Gain_{amplifier}\ Gain_{mixer}}} + \frac{1}{\frac{P1dB_{amplifier}}{Gain_{Mixer}}} + \frac{1}{P1dB_{mixer}}\right]^{-1} \tag{4.2}$$
$$= 10log_{10}[(\frac{1}{(1995.25)\,(60.256)\,(0.1361)} + \frac{1}{(0.2454)\,(0.1361)} + \frac{1}{1.2589})^{-1}]$$
$$= 10log_{10}(0.0325)$$
$$= -14.87dBm$$

Thus, the cascaded p1dB of the RF chain is -14.87 dBm.

4.4.3 IIP3 and OIP3

IIP3 or third order input intercept point and OIP3 or third order output intercept point are important parameters that are used to measure the linearity and distortion characteristics of electrical devices. IIP3 characterizes the point at which the inter-modulation products generated by the device reach the same power level as the desired signal. The input power level at which the distortion products become significant and start to affect the performance of the device is the IIP3 and the corresponding output power level is the OIP3. Equations 4.4 and 4.5 show the cascaded iip3 and oip3 equations, respectively.

$$IIP3_{cascaded} = 10log_{10}[\frac{1}{IIP3_{switch}} + \frac{G_{switch}}{(IIP3^{amplifier)}} + \frac{G_{switch}G_{amplifier]}}{(IIP3_{mixer})}]^{-1} \quad (4.3)$$

$$= 10log_{10}[\frac{1}{316227.766} + \frac{0.871}{1.584} + \frac{(0.871)(60.256)}{25.1188}]^{-1}$$

$$= 10log_{10}[2.6393]^{-1}$$

$$= 10log_{10}[0.3789]$$

$$= -4.214dBm$$

The cascaded iip3 of the system is -4.214dBm

$$OIP3_{cascaded} = 10log_{10}[\frac{1}{(G_{mixer}\,G_{amplifier}\,OIP3_{switch})} + \frac{1}{(G_{mixer}\,OIP3^{amplifier)}} + \frac{1}{(OIP3_{mixer})}]^{-1} \quad (4.4)$$

$$= 10log_{10}[\frac{1}{(60.256)(0.1361)(275422.87)} + \frac{1}{(0.1361)(50.118)} + \frac{1}{(3.419)}]^{-1}$$

$$= 10log_{10}[0.4391]^{-1}$$

$$= 10log_{10}[2.2774]$$

$$= 3.57dBm$$

The cascaded oip3 of the system is 3.57dBm

4.4.4 Noise Figure (NF)

Noise figure can be defined as the ratio between total output noise power and input noise power. Noise figure is a measure of how much a device adds noise to a signal when the signal goes through the device. Equation 4.6 shows the cascaded noise figure equation for a RF chain.

$$NF_{cascaded} = 10log_{10}(NF_{switch} + \frac{NF_{amplifier} - 1}{G_{switch}} + \frac{NF_{mixer} - 1}{G_{switch}\,G_{amplifier}}) \quad (4.5)$$

$$\begin{aligned} &= 10log_{10}(1.2023 + \frac{1.251 - 1}{0.871} + \frac{7.3451 - 1}{(0.871)\,(60.256)}) \\ &= 10log_{10}(1.2023 + 0.2870 + 0.1209) \\ &= 2.09dB \end{aligned} \quad (4.6)$$

So, the total cascaded NF of our RF chain is 2.09dB

4.5 MATLAB's RF Budget Analyzer Results

We used MATLAB's RF Budget Analyzer [7] to calculate the cascaded Gain, NF and OIP3 of the system. Figure 4.6 shows the RF Budget Analyzer results. The first block in the chain is a generic block used to emulate the RF switch, followed by the amplifier and then the de-modulator to emulate the mixer in our RF chain. We used the RF parameters of all the components in the RF chain from the data sheet of the respective components. The analyzer shows the cascaded gain, NF and OIP3 at different lengths of the chain and also for the full chain. The value shown by the analyzer matches our calculated results shown in previous section.

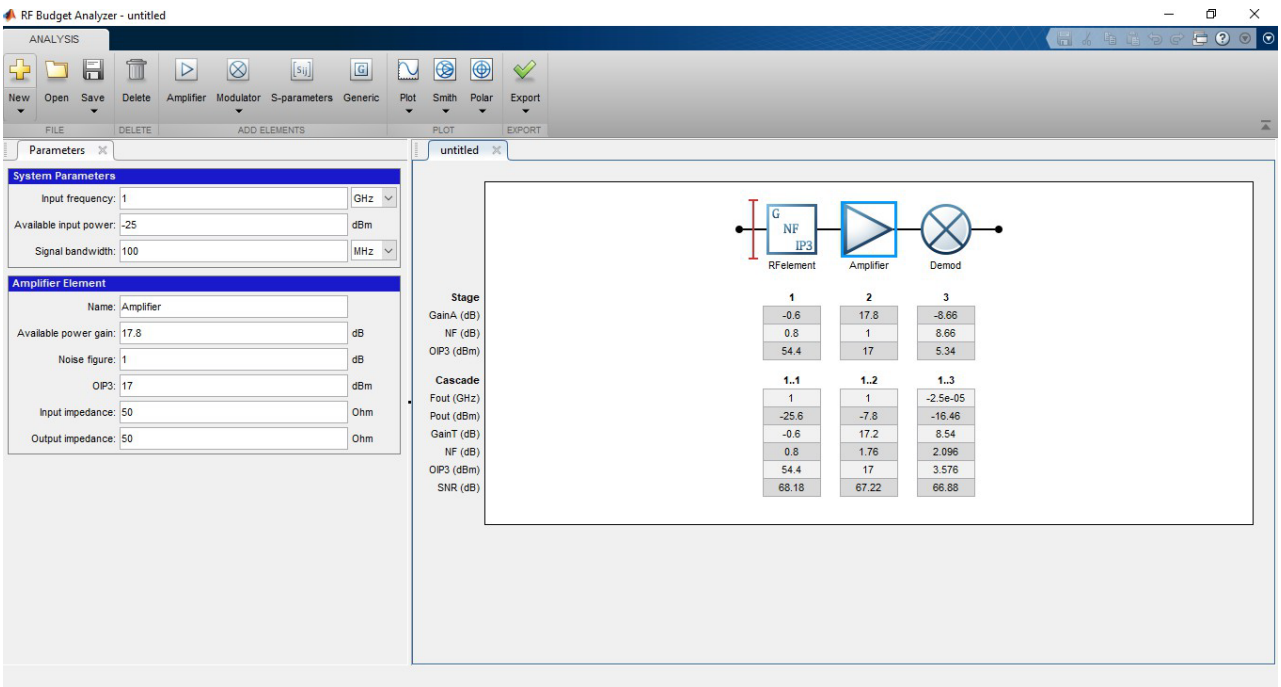

Figure 4.6: MATLAB's RF Budget Analyzer Results

Chapter 5: Simulation Results and RF Board Schematic and Layout

5.1 Simulation Setup

Figure 5.1 shows the simulation schematic for our simulations in AWR. For emulating the two PLLs we used two multi-tone sources. For all the frequencies we set the PLL harmonics that we found in table3.1 to emulate the PLL output .The mixer in schematic has the same specifications as given in the data-sheet for ADE30W+. The gain conversion and 1dB compression points for the mixer are modified each time according to the frequency we are simulating. The mixer is set to down-conversion mode. The load is matched to 50ohm. We placed three test points, one at the end of Rx/Tx PLL, one at the end of the reference PLL and one at the end of the mixer output. For all the simulations, the Rx/Tx PLL 1st harmonic power is set to 5dBm, and the reference PLL 1st harmonic power is set to 4dBm.

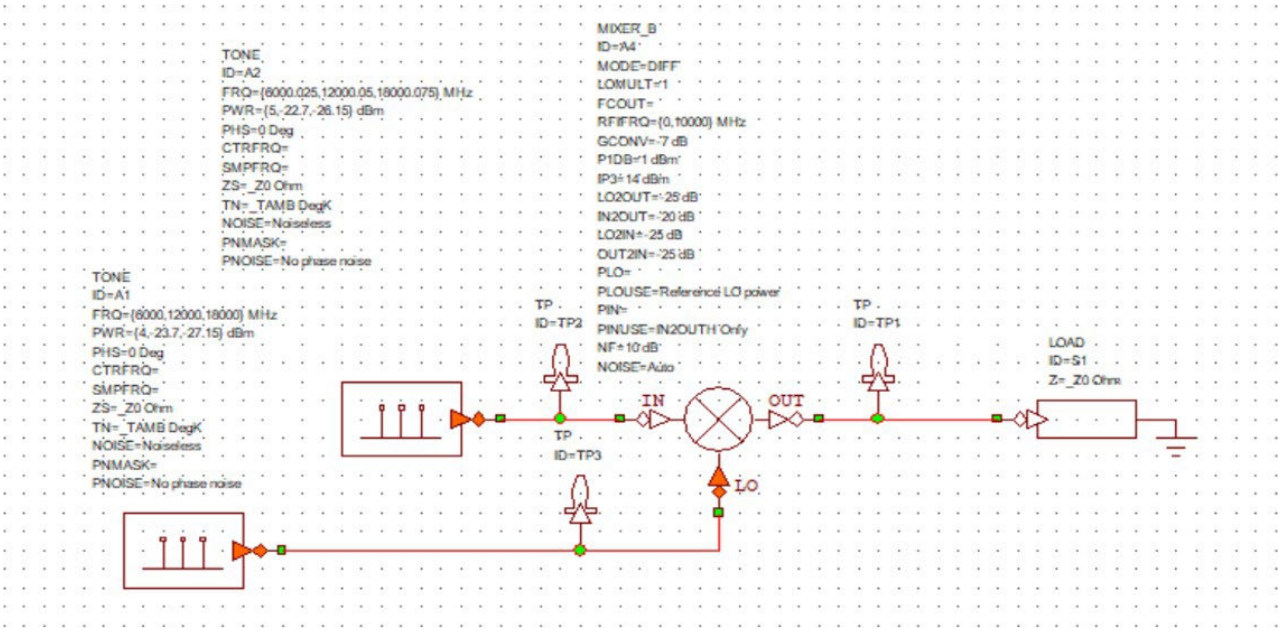

Figure 5.1: AWR System Schematic

5.2 0.6 GHz Simulation Results

Figure 5.2 shows the simulation results for a frequency of 0.6GHz. Figure 5.2ashows the Rx/Tx PLL output which is set to 0.600025GHz. The primary component of 5dBm can be seen at that frequency. The second harmonic and third harmonic at 1.200050 Ghz and 1.800075Ghz has the same value of 31.11dBc and 9.2 dBc as given in table 3.1. Figure 5.2b shows the reference PLL output set to 0.6 Ghz. The primary component of 4 dBm can be seen with the second and third harmonics of same power level as mentioned before. The output spectrum shown at figure 5.2c shows the main IF signal at 25kHz having a power of -5.99dBm. The 50kHz harmonic has a power of -50.35 dBm which will be further attenuated by 40 dB by the filter.

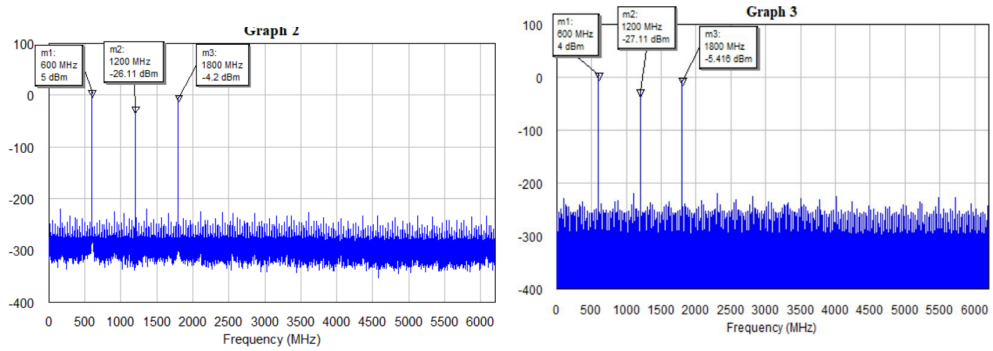

(a) PLL Rx/Tx Output (b) Reference PLL Output

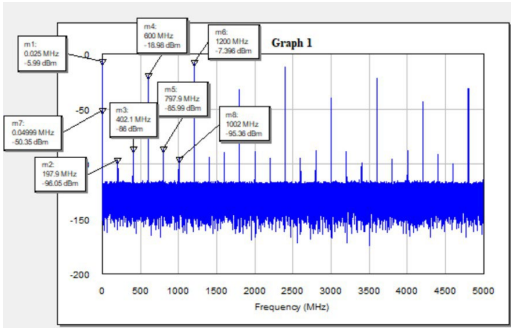

(c) Mixer Output

Figure 5.2: 0.6 Ghz simulation results

5.3 1 GHz Simulation Results

Figure 5.3 shows the simulation results for a frequency of 1 GHz. Figure 5.3a shows the Rx/Tx PLL output which is set to 1.000025GHz. The primary component of 5dBm can be seen at that frequency. The second harmonic and third harmonic at 2.00050 Ghz and 3.000075Ghz has the same value of 23.09dBc and 8.42 dBc as given in table3.1 . Figure 5.3b shows the reference PLL output set to 1 Ghz. The primary component of 4 dBm can be seen with the second and third harmonics of same power level as mentioned before. The output spectrum shown at figure 5.3c shows the main IF signal at 25kHz having a power of -8.366dBm. The 50kHz harmonic has a power of -48.01 dBm which will be further attenuated by 40 dB by the filter.

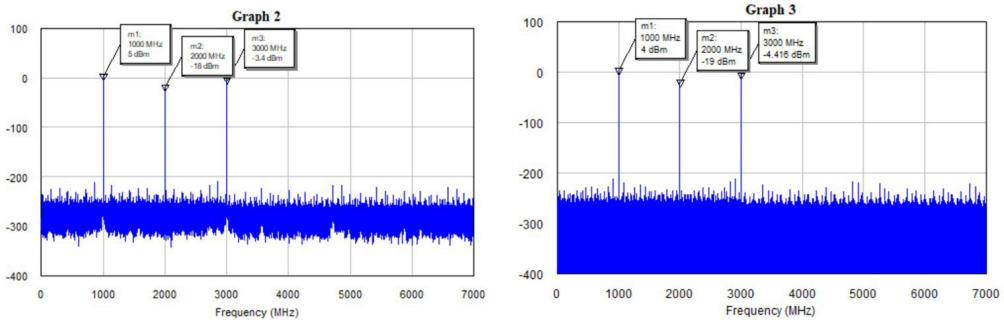

(a) PLL Rx/Tx Output (b) Reference PLL Output

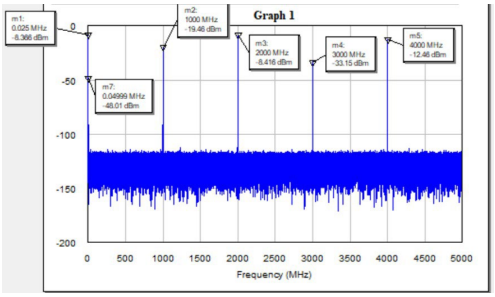

(c) Mixer Output

Figure 5.3: 1 Ghz simulation results

5.4 2 GHz Simulation Results

Figure 5.4 shows the simulation results for a frequency of 2 GHz. Figure 5.4a shows the Rx/Tx PLL output which is set to 2.000025GHz. The primary component of 5dBm can be seen at that frequency. The second harmonic and third harmonic at 4.00050 Ghz and 6.000075Ghz has the same value of 24.7dBc and 13.7 dBc as given in table 3.1 . Figure 5.4b shows the reference PLL output set to 2 Ghz. The primary component of 4 dBm can be seen with the second and third harmonics of same power level as mentioned before. The output spectrum shown at figure 5.4c shows the main IF signal at 25kHz having a power of -6.343dBm. The 50kHz harmonic has a power of -47.33 dBm which will be further attenuated by 40 dB by the filter.

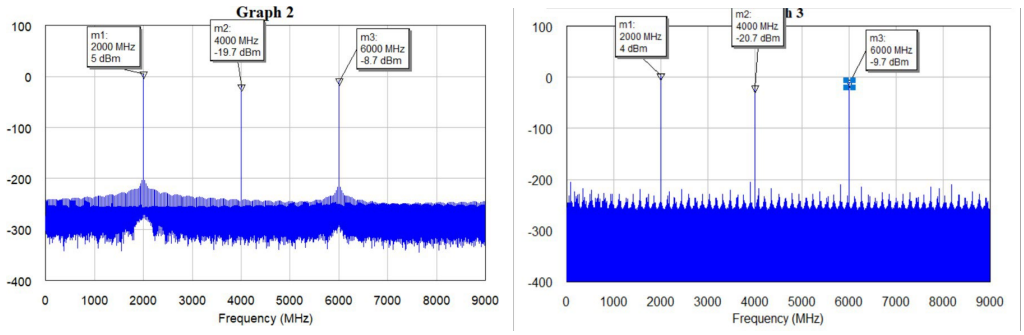

(a) PLL Rx/Tx Output (b) Reference PLL Output

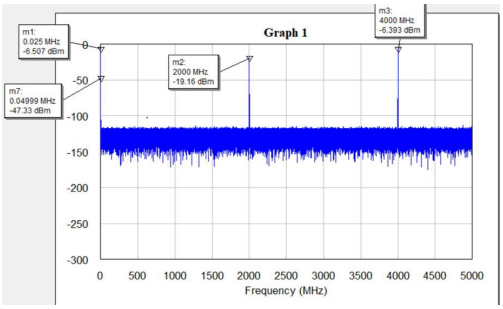

(c) Mixer Output

Figure 5.4: 2 Ghz simulation results

5.5 3 GHz Simulation Results

Figure 5.5 shows the simulation results for a frequency of 3 GHz. Figure 5.5a shows the Rx/Tx PLL output which is set to 3.000025GHz. The primary component of 5dBm can be seen at that frequency. The second harmonic and third harmonic at 6.00050 Ghz and 9.000075Ghz has the same value of 27.35dBc and 25.65 dBc as given in table3.1 . Figure 5.5b shows the reference PLL output set to 3 Ghz. The primary component of 4 dBm can be seen with the second and third harmonics of same power level as mentioned before. The output spectrum shown at figure 5.5c shows the main IF signal at 25kHz having a power of -6.343dBm.

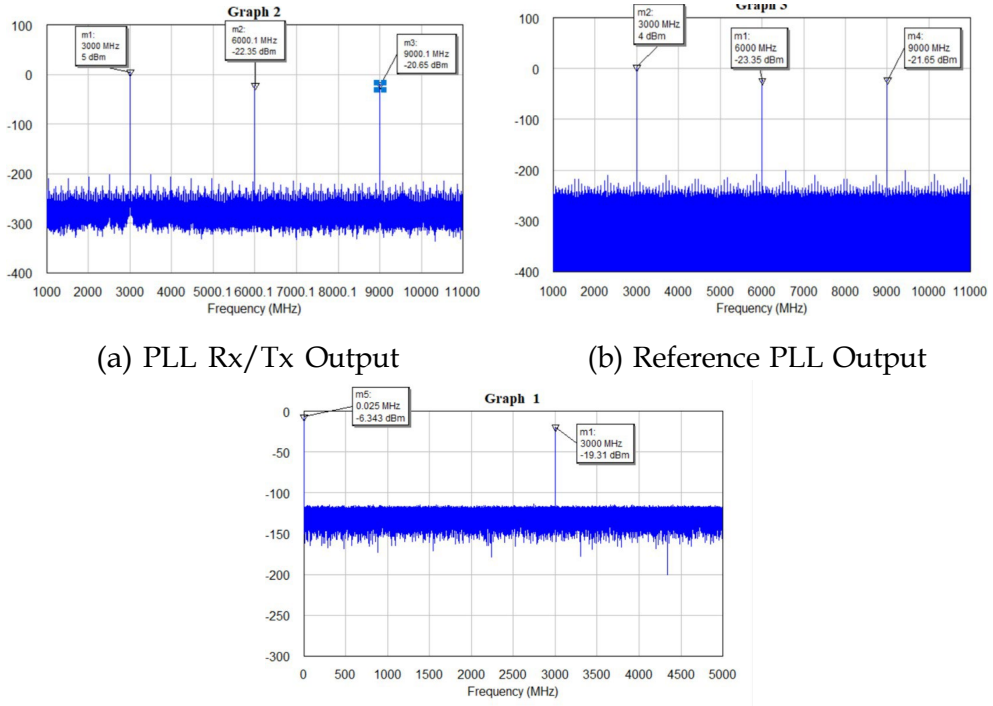

(a) PLL Rx/Tx Output (b) Reference PLL Output

(c) Mixer Output

Figure 5.5: 3 Ghz simulation results

5.6 4 GHz Simulation Results

Figure 5.6 shows the simulation results for a frequency of 4 GHz. Figure 5.6a shows the Rx/Tx PLL output which is set to 4.000025GHz. The primary component of 5dBm can be seen at that frequency. The second harmonic and third harmonic at 8.00050 Ghz and 12.000075Ghz has the same value of 33.6 dBc and 30.8 dBc as given in table3.1 . Figure 5.6b shows the reference PLL output set to 4 Ghz. The primary component of 4 dBm can be seen with the second and third harmonics of same power level as mentioned before. The output spectrum shown at 5.6c shows the main IF signal at 25kHz having a power of -6.367dBm.

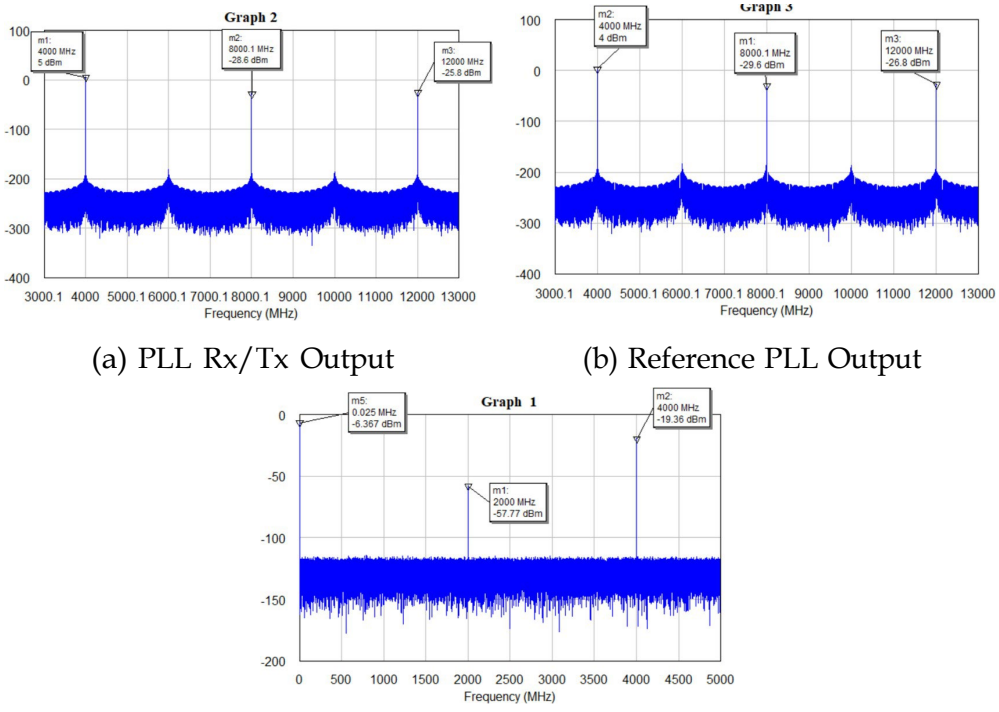

(a) PLL Rx/Tx Output

(b) Reference PLL Output

(c) Mixer Output

Figure 5.6: 4 Ghz simulation results

5.7 RF Board Schematic and Layout

In this section we discuss the schematic and layout of the RF board. Figures 5.7 and 5.8 show the schematic and the layout of the board. Table 5.1 shows the entire stack up of the board with each layer material and thickness We have used cadence OrCAD Capture and PCB Editor for the schematic and layout, respectively. The footprints of all the components are drawn using pad stack editor. For the input signals coming from the two PLL s and the antenna and the output IF signal coming out of the filter, we have used SMA connectors (part number-142-0701-801). Digital signals V1 and V2 needed to be supplied to the RF switch and the LDO input voltage we have used a connector U44 (part number-5031590501). All RF components have been grounded to RF ground and all other digital components are ground to digital ground. It is a three-layer board. The first layer has been used for routing.

A few routing lines are also drawn in third layer which are connected with the footprint of the ICs using vias. The second layer is dedicated for RF ground which is shown in red. The third layer is used for digital ground which is shown in blue. The digital and RF grounds are isolated from one another by using a ferrite bead (U57 in schematic). One pad of the bead is connected to RF ground layer by a via going from first layer to second layer. The other pad of the bead is connected to the digital ground layer by a via going from first to third layer. The SMA connectors (U52, U53, U54, U55, U56) have 4 rf ground pads each with two pads on the first layer and two pads on the bottom layer. All these pads are connected to the second layer using vias. The board dimensions are 48mm by 38mm. Table 5.1 shows the RF board stack up.

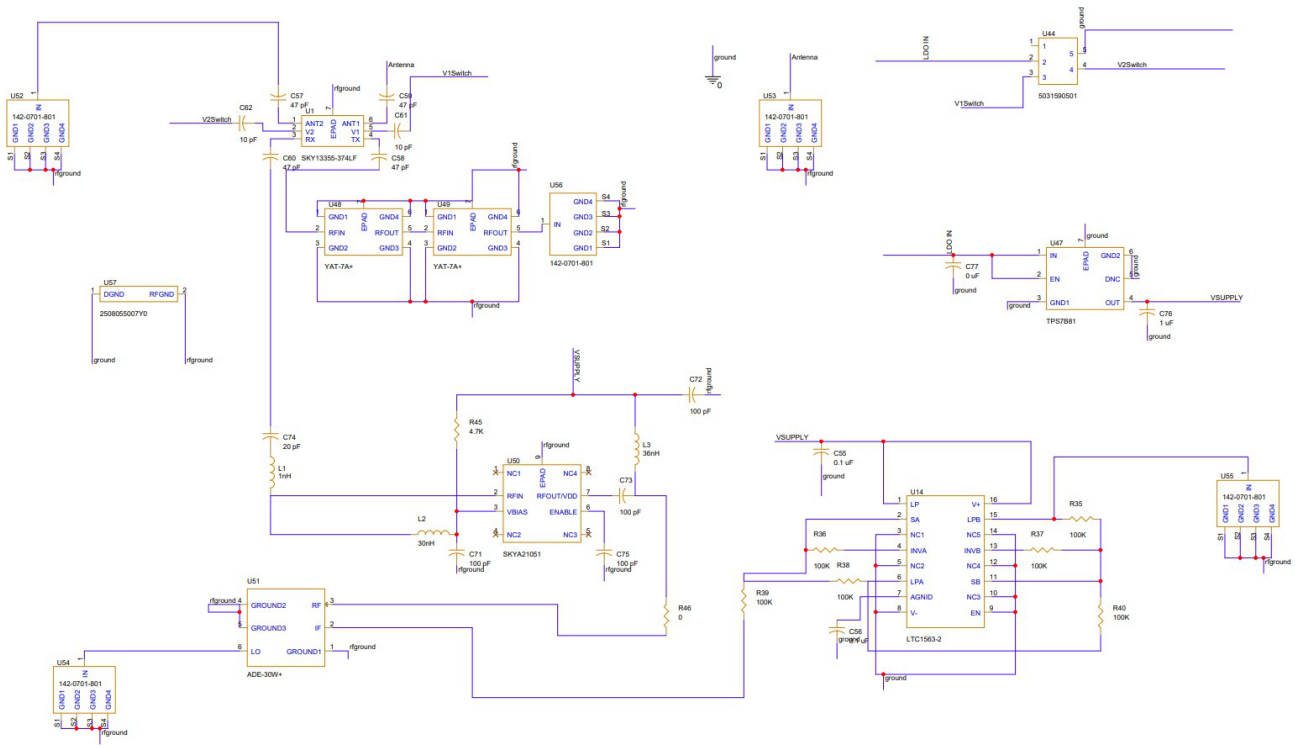

Figure 5.7: RF Board Schematic

Layer Name (From Top)	Thickness (In mm)	Material
Conductor 1	0.03048	copper
Dielectric 1	0.2032	FR-4
Conductor 2	0.03048	copper
Dielectric 2	0.2032	FR-4
Conductor 3	0.03048	copper

Table 5.1: RF Board Stack Up

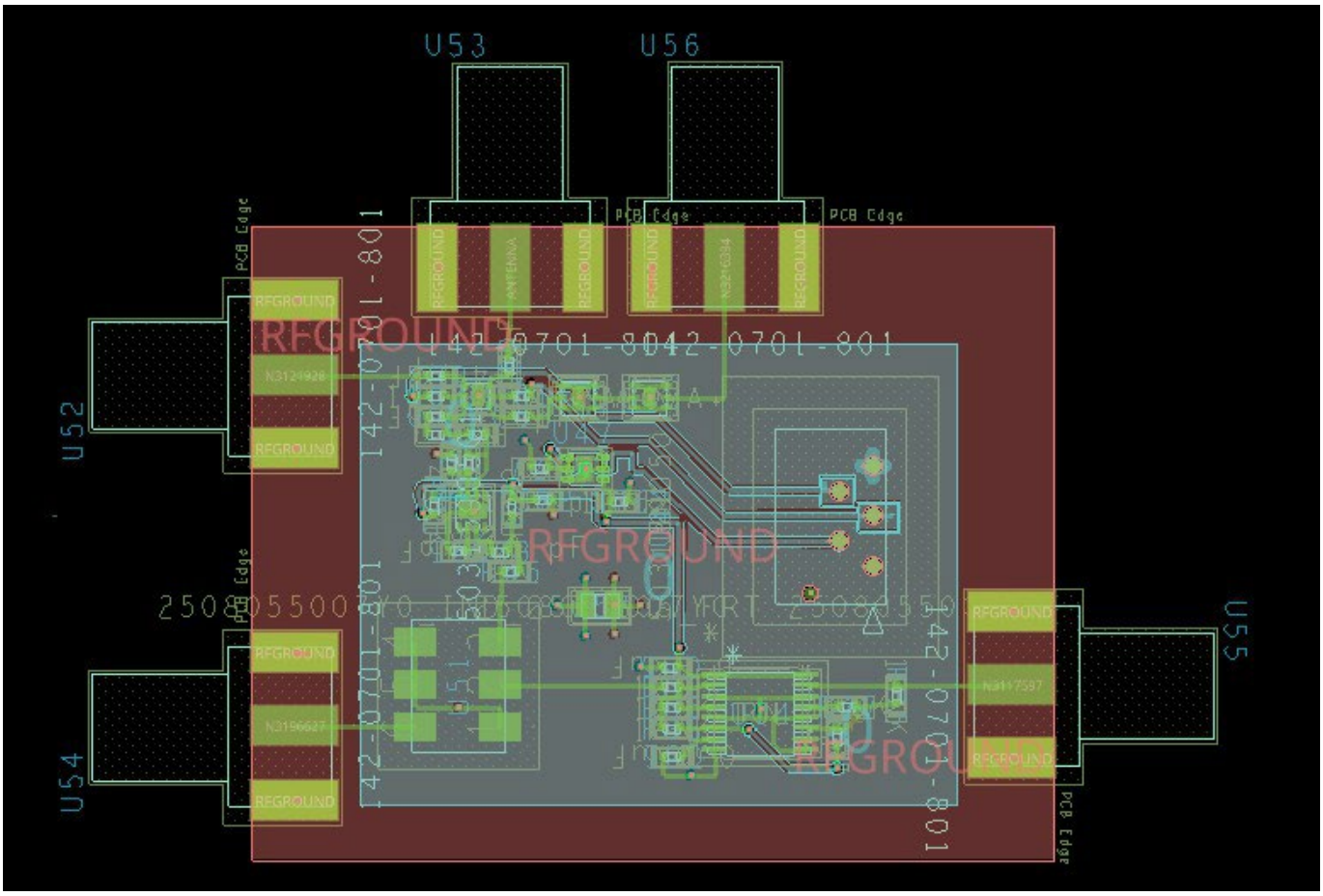

Figure 5.8: RF Board Layout

Chapter 6: Conclusion

The thesis presents the motivation, concept and design of the RF board which will be used as modular frequency array element for different applications. In chapter 1 and chapter 2 we present the introduction and background work ,literature review of the idea respectively. Chapter 3 focuses on the design specifications of the board and discusses the performance of the different components of the board and also the reason behind choosing each component namely , PLL , DPDT switch, filter, mixer, amplifier, LDO , ADC and antenna. Chapter 3 also presents the microstrip calculations which would be needed while routing the lines in final layout of the board. Chapter 4 presents the analysis of the design namely , RF budget calculations for both scenarios of module acting as a transmitter and a receiver .The calculations of cascaded gain , IIP3, OIP3, P1dB of the system are also shown. All calculations are verified in MATLAB Simulink and RF Budget analyzer tool. Chapter 5 shows the simulation results of the RF system at different frequencies in cadence AWR to see if the filter used in the board can attenuate the higher harmonic signals sufficiently. Chapter 5 also presents the schematic and layout of the RF board. In this concluding chapter we would conclude the thesis after discussing the summary of the results shown in chapter 5 and the directions for future research for this project.

6.1 Summary of the Results

In this section we are going to present a discussion on the simulation results shown in chapter5 and how to interpret those results. The purpose of running the simulations for the mixer network with multi tone sources in cadence awr at different frequencies was to find out the power of higher harmonics that are produced by the nonlinear PLL output. The multi-tone source is used to emulate the PLLs with the higher harmonics. The mixer has been given the same specifications as that of the ADE30W+ mixer which we are using in our board. The output spectrum produced shows the power level of all the signals produced by the mixer. Based on the power level of the higher harmonic signals we can decide on the attenuation expected to be given by the filter so that the higher harmonic signals almost come to the noise floor level after passing through the filter. From the simulations we found out the highest power of the second harmonic at 50kHz is -47.33 dBm at 2GHz. The filter that we are using, provides an attenuation of 70.2dB at 50kHz which is sufficient to push the higher harmonic signals almost to the noise floor level of the system.

6.2 Directions for Future Research

The aim of this research was to build a modular array system which can be used for different medical applications. We have designed the RF block of the array. We would be testing the board once it is manufactured. Further work is needed to build a digital board which would be interacting with the RF block presented in this thesis. Furthermore, there needs to be a clock distribution system when we would be making an actual system with arrays in it. Depending on the application the arrays would need to be arranged accordingly to optimize the received signal for accurate imaging.

Appendix A: PLL Harmonics

The data that was used to produce the table in 3.1 is taken from the data sheet of PLL MAX2871 which is given below.

https://www.analog.com/media/en/technical-documentation/data-sheets/MAX2871.pdf

Appendix B: RF Parameters of Different Components

The data that was used to produce the table in 4.1 and used in figure 4.2 and 4.1 is taken from the datasheet of each individual components which are listed below.

Switch - https://www.skyworksinc.com/-/media/SkyWorks/Documents/Products/501-600/201341C.pdf

Amplifier - https://www.skyworksinc.com/-/media/SkyWorks/Documents/Products/2801-2900/SKYA21051_203831C.pdf

Mixer - https://www.minicircuits.com/pdfs/ADE-30W+.pdf

Bibliography

[1] Abdulrahman. S. M. Alqadami, Anthony E. Stancombe, Konstanty S. Bialkowski, and Amin Abbosh. Flexible meander-line antenna array for wearable electromagnetic head imaging. *IEEE Transactions on Antennas and Propagation*, 69(7):4206–4211, 2021.

[2] Abdulrahman SM Alqadami, Anthony E Stancombe, Konstanty S Bialkowski, and Amin Abbosh. Flexible meander-line antenna array for wearable electromagnetic head imaging. *IEEE Transactions on Antennas and Propagation*, 69(7):4206–4211, 2020.

[3] E.J. Barlow. Doppler radar. *Proceedings of the IRE*, 37(4):340–355, 1949.

[4] Bart H Bijnens, Maja Cikes, Piet Claus, and George R Sutherland. Velocity and deformation imaging for the assessment of myocardial dysfunction. *European Journal of Echocardiography*, 10(2):216–226, 2009.

[5] Daniela Foll, Bernd Jung, Elfriede Schilli, Felix Staehle, Annette Geibel, Jurgen Hennig, Christoph Bode, and Michael Markl. Magnetic resonance tissue phase mapping of myocardial motion: new insight in age and gender. *Circulation: Cardiovascular Imaging*, 3(1):54–64, 2010.

[6] PAUL G HUGENHOLTZ, R Curtis Ellison, CHARLES W URSCHEL, ISRAEL MIRSKY, and EDMUND H SONNENBLICK. Myocardial force-velocity relationships in clinical heart disease. *Circulation*, 41(2):191–202, 1970.

[7] Bircan Kamislioglu and Ayhan Akbal. A new rf budget analysis and rf measurement testbench application. In *2018 International Conference on Artificial Intelligence and Data Processing (IDAP)*, pages 1–5, 2018.

[8] Richard P Lewis, SE Rittogers, WF Froester, and HARIsIOs Boudoulas. A critical review of the systolic time intervals. *Circulation*, 56(2):146–158, 1977.

[9] DEAN T MASON, EUGENE BRAUNWALD, JAMES W COVELL, EDMUND H SONNENBLICK, and JOHN ROSS JR. Assessment of cardiac contractility: the relation between the rate of pressure rises and ventricular pressure during isovolumic systole. *Circulation*, 44(1):47–58, 1971.

[10] Kasper Sørensen, Samuel E Schmidt, Ask S Jensen, Peter Søgaard, and Johannes J Struijk. Definition of fiducial points in the normal seismocardiogram. *Scientific reports*, 8(1):15455, 2018.